

11-37-ER
3030
P. 71

MAGNETOSTRICTIVE DIRECT DRIVE MOTORS

By

Dipak Naik

P.H. DeHoff, P.I.

Semi-Annual Report

January 1, 1990 - June 30, 1990

NASA Grant NAG 5-1169

Department of Mechanical Engineering & Engineering Science

University of North Carolina at Charlotte

Charlotte, NC 28223

(NASA-CR-186895) MAGNETOSTRICTIVE DIRECT
DRIVE MOTORS Semiannual Report, 1 Jan. - 30
Jun. 1990 (North Carolina Univ.) 71 p
CSCL 131

N90-28855

Unclas
G3/37 0308272

MAGNETOSTRICTIVE DIRECT DRIVE MOTORS

ABSTRACT

This study is concerned with developing magnetostrictive direct drive research motors to power robot joints. These type motors are expected to produce extraordinary torque density, to be able to perform microradian incremental steps and to be self-braking and safe with the power off. Several types of motor designs have been attempted using magnetostrictive materials. In this report one of the candidate approaches (the magnetostrictive roller drive) is described. The method in which the design will function is described as is the reason why this approach is inherently superior to the other approaches. Following this, the design will be modelled and its expected performance predicted. This particular candidate design is currently undergoing detailed engineering with prototype construction and testing scheduled for mid 1991.

<u>Sr. No.</u>	<u>Contents</u>	<u>Page No.</u>
	NOMENCLATURE	ii-v
	LIST OF FIGURES	vi
	LIST OF TABLES	vii
1	Introduction	1
2	Construction	1
3	Principles of Operation	1
4	Expected Performance	2-25
	4.1 Basic Kinematics	2
	4.2 Torque	11
	4.2.1 Drive Rods	11
	4.2.2 Structural Stresses and strains	12
	4.3 Speed/Acceleration/Step Resolution	15
	4.3.1 No Load Frequency Response	15
	4.3.2 On Load Frequency Response	17
	4.4 Temperature	18
	4.4.1 Coil Losses	19
	4.5 Designing For Wear	20
	4.5.1 Effect of Design Variables	21
	4.5.2 Effective Wear Control	21
	4.5.3 Wear Prediction Technique	22
	4.5.4 Analytical Technique	23
	4.5.5 Wear Calculations for Drive Cam	25
	4.6 Closure	25
	APPENDIX: A Preliminary Drawings for Prototype B	41-60
	REFERENCES	61

NOMENCLATURE

A = contact area (apparent) in wear calculations
a = distance between end of drive drum to the point of application of normal forces
a_{lin} = linear acceleration (ft/sec²)
B = magnetic flux density
B_{air} = magnetic flux density in air
B_{st} = magnetic flux density in steel
b = width of rectangular contact area for Hertz contact stresses
b₁₂ = width of rectangular contact area for drive roller & drive cam
b₂₃ = width of rectangular contact area for drive roller & drive shaft
c = width of load support in rolling direction
D = constant in deflection calculations
D₁ = diameter of drive cam
D₂ = mean diameter of drive roller
D₃ = diameter of drive shaft drum
D_{odr} = effective lever arm of drive shaft drum
D_{dr} = rod lever arm
d = sliding distance in wear calculations
d_t = diameter of Terfenol rod
d_L = distance over which force F acts
d_{WH} = total energy stored in a steady magnetic field
d_{incoil} = inner diameter of magnetic coil for drive rollers
d_{ocoil} = outer diameter of magnetic coil for drive rollers
d_{air} = length of air gap
E = Young's modulus
F = Force
F_d = rod drive force
F_{pl} = spring preload force
F_{fb} = Radial bearing frictional force opposing spring preload force
F_{np1} = Normal force caused by seating of bearing
F_{rz} = Resultant frictional force opposing roller removal in z direction
F_{fpl} = Friction force in seating which opposes the preload
F_{fp1} = Friction force after seating which opposes roller removal
F_s = average force of drive roller return spring.
F_z = forces in Z direction
f_{op} = operating frequency of motor
f_c = critical frequency of Terfenol rods
f_{nl} = no load frequency of motor
f_{ol} = on load frequency of motor
G = drive force on drive shaft drum (lbs)
G_v = required lift
G_r = total possible radial gap
H = material hardness

H_{cu1} = copper loss for electromagnetic coil
 H_{cu2} = copper loss for Terfenol rod coil
 H_{co1} = core loss for electromagnetic coil
 H_{co2} = core loss for Terfenol rod coil
 h = depth of wear perpendicular to the contact area
 h_1 = depth of wear at the center of worn area on body 1
 h_2 = depth of wear at the center of worn area on body 2
 h_t = total depth of wear at the center of worn area on body 1
 and 2
 I = electric current
 I_1 = current in electromagnetic coil
 I_2 = current in Terfenol rod coil
 J = polar moment of inertia
 J_{osc} = polar moment of inertia of oscillating members of
 motor
 J_{rot} = polar moment of inertia of rotating members of motor
 j = film thickness
 K_m = wear coefficient
 K_D = K factor in contact stress calculations
 K_{D1} = K factor for roller in the drive cam
 K_{D2} = K factor for roller on drive shaft drum
 L = Load in wear calculations
 l_{dr} = length of drive drum
 M_o = moment acting on drum in inch lbs per linear inch
 m = mass of drive roller
 N_{cam} = normal force on drive cam
 n = no of times surface passes through loaded area
 P = contact pressure in wear calculations
 p_c = load for contact stress calculatins
 p_{dr} = total load on drive drum in lbs per linear inch
 p_r = load on roller in lbs per linear inch
 R = radius of drive drum
 r_{coil} = center point (location of slot) for electromagnet
 coil for drive rollers
 r_{incoil} = inside radius of electromagnet coil for drive
 rollers
 r_{ocoil} = outside radius of electromagnet coil for drive
 rollers
 R_c = radius from centre of motor to centre of drive roller
 r_{dr} = drive drum radius
 R_{air} = reluctance of air gap in magnetic circuit
 R_{coil1} = electrical resistance of electromagnetic coil
 R_{coil2} = electrical resistance of Terfenol rod coil
 r_{rod} = rod lever arm (in)
 r_r = drive roller mean radius
 S = core cross sectional area
 S_{air} = cross sectional area of air gap
 S_{st} = cross sectional area of steel core
 s = amount of drive roller arc length travel required during
 the return stroke.
 T_{dr} = drive torque (ft-lbf)

T = Temperature
 T_{op} = time period of motor
 T_{nl} = no load time period of motor
 T_{ol} = on load time period of motor
 t_{dr} = thickness of drive drum
 t = time
 t_1 = time of first observation
 t_2 = time of second observation
 U = rolling velocity
 U_s = sliding velocity
 V = Velocity
 V_m = magnetomotive force
 W = wear
 W_r = rate of wear
 W_1 = wear at time t_1
 W_2 = wear at time t_2
 y_r = radial deformation of drum

Greek Alphabets:

α = angular acceleration (radians/sec²)
 α_{en} = environmental effects
 α_{nl} = no load angular acceleration of motor
 α_{ol} = on load angular acceleration of motor
 β = geometric effects
 θ = angular resolution of motor
 ν = poisson's ratio
 ψ = cam angles
 Φ = magnetic flux
 ϕ = roller angle
 ϕ_f = finish factor
 Ω = electrical resistance in ohms
 μ_0 = permeability of free space
 μ_s = coefficient of sliding friction
 λ = constant
 ΣF_z = sum total of forces in Z direction
 ΣJ = total polar moment of inertia of oscillating and
rotating members of motor
 ΣJ_{osc} = total polar moment of inertia of oscillating members
of motor
 ΣJ_{rot} = total polar moment of inertia of rotating members of
motor
 $\Sigma Loss$ = total heat loss in motor

ΔL_{dr} = expansion of drive rods

Δr_{dr} = total radial deformation of drive shaft drum, drive
rollers and drive cam

Δr_r = radial deformation of drive roller

ΔL_{dr} = expansion of drive rods

σ_{cmax} = Maximum contact stress

Abbreviations/Acronyms:

rpm = revolutions per minute

CW = clockwise

CCW = counter clockwise

AWG = American wire gage

LIST OF FIGURES

<u>Sr. No.</u>	<u>Title</u>	<u>Page No.</u>
1	Magnetostrictive Direct Drive Motor	26
2	Top View of Motor	27
3	Front View of Motor (Section A-A)	28
4	Locking roller Drive Details	29
5	Output Shaft Drum	30
6	Drive Drum	31
7	Functional Operation of Roller Drive	32
8	Free Body Diagram of Rollers	33-34
9	Guide Spring Details	35
10	Regions of Backlash, Dead Zones and Hysteresis	36-38
11	Performance Characteristics of FSZM Terfenol Rods	39
11	Effect of Operational Variables on Wear Rate	40

LIST OF TABLES

<u>Sr. No.</u>	<u>Title</u>	<u>Page No.</u>
1	Radial Deformation of Drive Drum	13
2	Radial Deformations of Drive Rollers	14
3	Radial Deformations of Drive Cam and Drive Shaft Drum	14
4	Cumulative Radial Structural Deformations	14
5	Contact Stresses:	15
	a. Drive Roller In Drive Cam	
	b. Drive Roller On Drive Shaft Drum	
6	Polar Moment of Inertia (J_{osc}) of Oscillating Members	17
7	Polar Moment of Inertia (J_{rot}) of Rotating Members	18
8	Polar Moment of Inertia (ΣJ) of Oscillating and Rotating Members	18
9	On Load Angular Accelerations and Frequency Response	18
10	Electromagnet Coil Specifications	19
11	Coil Wire Specifications	19
12	Terfenol Rod Coil Specifications	19
13	Heat Losses in Coils	20

MAGNETOSTRICTIVE ROLLER DRIVE MOTOR

John M. Vranish

Dipak P. Naik

NASA/Goddard Space Flight Center

1. INTRODUCTION

Robot arms in space are currently powered by low torque, high speed electric motors which use transmissions as a means of torque multiplication and which utilize brakes as a safety device when the power is off. Direct drive control, though highly desirable, is not presently practical. The addition of the transmission hardware and brakes makes the system bulky and inefficient. Also, the fact that DC motor servo control is used, results in limit cycling. Motors based on magnetostrictive principles appear to hold promise in alleviating these problems and to allow for unprecedented precise microradian steps, safety and agility. Several concepts based on magnetostrictive drives have been attempted, all with varying degrees of success. In this paper the magnetostrictive roller drive motor will be introduced and its means of functioning explained. The reasons why this new design is inherently superior to earlier magnetostrictive motors will be made clear.

2. CONSTRUCTION

Fig. 1 illustrates the motor concept. It essentially consists of magnetostrictive drive rods which impart a torque to the roller locking mechanism which, in its turn, transfers the torque to the output shaft. The torque produced by the magnetostrictive rods is oscillatory while that emerging from the output shaft is unidirectional (but reversible). Figs. 2 and 3 show the proposed design in full scale and give an idea of its size and complexity. The locking roller drive is the heart of the motor and Fig. 4 shows details of this mechanism. Figs. 5 (drive shaft drum) and 6 (drive drum) show the main components.

3. PRINCIPLES OF OPERATION

Figs 2 and 3 show a full scale view of the proposed motor design. We expect approximately 60 ft-lbs torque with no-load speeds on the order of 10 rpm from the motor.

Fig. 7 illustrates the functional operation of the roller drive. The illustration shows clockwise drive shaft rotation. Each of one pair of magnetostrictive rods (A) expands approximately 0.001in/in. with great force, exerting 2 ksi (500 lbs each for a 0.55 in diameter rod) under the influence of a magnetic field. The opposing rods (B) contract

approximately 0.001 in./in. each. Thus we have a rotational motion of the drive drum. This drive drum is coupled to the drive shaft drum by conical rollers. These rollers are lightly preloaded so there is no backlash between the drive cam and the drive shaft drum. As the drive drum rotates CW, the CW drive rollers try to roll up the CW drive cam on the drive drum; but are immediately pinned between the drive shaft drum and the drive cam. And since $\tan \psi < \mu$ the frictional force preventing sliding builds up instantaneously so the rollers lock. This locking sets up reaction forces in the drive drum and the drive shaft drum. These forces, in turn, create the friction forces on the drive shaft drum which constitute the source of motor torque. At the same time, the magnets above the CCW rollers are activated. Following this, the CCW rollers first roll, disengaging from both the drive cam and the drive shaft drum, and then are each pulled up against the magnetized plate. Thus, a preferential CW torque and motion is established. When the magnetic field in the expanding rod set (A) collapses, the system returns to neutral and the cycle can start again (except that the CCW rollers are effectively nonparticipatory). When the magnetic field is excited at high frequency (on the order of 400 Hz) the system cycles in a rapid ratcheting motion and we get relatively high rpm (10 rpm for a single stage motor). When the above procedure is followed using the magnetostrictive rod pair (B) as the drive source, and another set of rollers which are stationed underneath the first set of conical rollers. The drive cams on the drive drum are set up so that locking takes place in CCW motion and we get CCW ratcheting motion.

4. EXPECTED PERFORMANCE

In this section we will examine the expected performance of the motor. We will first investigate how the system works kinematically. This will ensure that the basic motion sequence of the device is correct. We will next analyze the device to see that it will produce the required torque. Then we will estimate its potential with respect to speed, acceleration and step resolution. This, in turn, will be followed by an estimation of the power, efficiency and operating temperature of the system. Finally, wear and longevity will be estimated.

4.1 Basic Kinematics

In this section we will examine the basic kinematics of the motor. We will go through all the steps of the drive cycle first in one direction and then in the other, tracing the movements of all critical parts as we go.

We will begin by driving the motor clockwise. For the motor to operate with such small drive strokes, components

must be kept in contact and forces in balance at all times with backlash, hysteresis and dead zones reduced to a minimum. Fig. 8 (a) and (b) shows the preload forces in the X-Y plane. The CW rollers remain in contact with both the drive cam and the drive shaft drum throughout the power stroke. Each roller rolls initially, causing structural deformation, until the driving force builds up to equal the torque opposing the motor shaft. Then the CW rollers lock the drive cam and the drive shaft drum together and the motor overpowers the torque load on its shaft. During the relaxation stroke, the drive drum rotates CCW relative to the drive shaft drum. This forces the CW rollers to rotate CCW until all deformations are relieved and the forces shown in Figs. 8 (a) and (b) return to preload levels. This also places each roller in contact with its guide spring/bearing (Fig. 9). As the drive drum continues to move CCW, each guide spring/bearing pushes its respective roller before it. These rollers, however, are preloaded against the drive cams and the drive shaft drum, so they roll throughout the return stroke. This leaves them each in contact with the drive cams and drive drum so backlash and dead zones are minimized for the next power stroke. When we choose to reverse directions, we release the magnets above the CCW rollers and excite those above the CW. We then excite the magnetostrictive rods to perform a CCW power stroke. The CCW rollers respond to their preload springs and move down in the Z direction until they contact the cams of the drive drum and the drive shaft drum, where they begin the process of first rolling to build up torque forces and then locking the drive drum and drive shaft drum together. The CW rollers roll until all deformations and forces are reduced to preload minimum. They then are pulled up against their respective magnets and CCW ratcheting can be performed. But how do we keep this balance of forces and minimum backlash and dead zones throughout the motor life, when wear is occurring and when the drive drum and the drive shaft drum are slightly out of round?

A second cam surface is used along with vertical preload springs to provide an independent suspension for each of the rollers. Thus, they can individually stay in contact with the drive drum cam and the drive shaft drum, minimize backlash and maintain balance of forces despite wear and anomalies in manufacture. Again, $\tan \psi < \mu$ so the drive rollers will not displace in the Z or vertical direction no matter how much force is applied. For the CCW rollers, separation is desired throughout the power and relaxation strokes. Without this separation, a relaxation stroke would not be possible. Thus, electromagnets are used to lift the CCW rollers clear of contact with the drive drum cams and drive shaft drum during the CW ratcheting process. For CCW ratcheting, we excite the electromagnets over the CW rollers and relax those over the CCW rollers. We will now identify areas of dead zones, backlash and hysteresis.

In Fig.10, we identify the regions of back lash, dead zones and hysteresis. In Fig. 10 (a), we trace the contact stresses build-up on the drive roller throughout the drive stroke. When the drive stroke is just beginning, the stress on the drive roller is that caused by the downward preload and is minimal. As the power stroke continues, the drive roller rolls and deforms both itself and the surrounding structure (see also Fig.10 (b)) until the torque opposing the motor is equalled (see Fig. 10 (c)). At this point, the drive rollers stop rolling, they lock the drive cam and the drive shaft drum together and the drive shaft turns. The graphs of Figs.10 (a) and 10 (b) show the contact stresses and deformations associated with maximum torque. We have set as a rule-of-thumb that this should occur before one half of the stroke because we want reasonable movement of the load even under high torque conditions. The portion of the drive stroke during which the rollers roll and the structure deforms up to the point of movement of the drive shaft represents the dead zone. The extent of the dead zone is proportional to the torque load of the motor. For a low torque loading, the dead zone will be small, the stroke relatively long and the speed relatively high. During the return stroke (Fig.10 (a) and (b)), the drive rollers first roll CCW to relieve the forces and deformations until each is in contact with its guide spring/bearing. At this point, this spring, which is attached to the drive cam, forces the drive rollers to follow the drive drum and, together with the Z direction preload springs, forces contact between each of the drive rollers and the drive cam and drive shaft drum. Thus the drive rollers roll CCW throughout the return stroke. And, because of the shape of the cams they remain in the same relative Z position throughout. In certain circumstances, where speeds are high enough, the inertia of each drive roller during the return stroke loads its guide spring/bearing slightly, and opens a tiny gap between the drive roller and the drive cam and drive drum. The drive roller preload spring forces each drive roller in the Z direction until contact is re-established. But this places the roller on a slightly different point on its drive cam and leaves each guide spring/bearing with a slight preload. This, in turn, loads forces and deformations into each roller, drive cam and drive shaft drum. But this preload, in turn, improves the system frequency response until the gap no longer occurs. This phenomenon is termed "walking" and the difference between the forces and deformations in the system under this condition and normal preload is hysteresis. When we go from CW drive to CCW drive, this hysteresis is negated. Under starting conditions of normal preload (no walking effects), there is no inherent backlash. Both sets of rollers are at preload and the magnets above one set of rollers pulls them up and the CCW drive rollers begin to generate torque and deformations immediately. Where walking effects have occurred (say during CW operation) and we begin operating CCW, the following

sequence occurs. First the magnets above the CW rollers are excited and those above the CCW rollers relaxed. The CCW rollers are moved by their preload springs so that each engages its drive cam and the drive shaft drum at normal preload. The CW rollers, however, are each held in place by residual "walking" forces from its guide spring/bearing and cannot respond to its lifting magnet. These residual forces must be relieved and the rollers lifted before the motor can ratchet in a CCW direction. As the CCW power stroke begins, the CCW rollers begin to roll immediately, building up deformations and torque in the system. At the same time, the CW rollers roll down their drive cams (rotating CCW) and relieving the stresses caused by the walking effect. Once normal preload levels are reached, their magnets pull them up and normal CCW operation commences. The period during which the walking effect forces exceed the forces caused by the CCW rollers is a period in which no CCW motion or torque can be generated and adds to the backlash.

We will also briefly examine how the system behaves kinematically during the return stroke (say CW). Under these circumstances, the Terfenol rods are returning CCW to neutral and the CCW drive rollers are disengaged. In this instance, each CW roller will rotate CCW because of its preload contact with its drive cam and the drive shaft drum. Because of the directional difference of rotation between the drive drum cams and the drive shaft drum and because of the reverse slope of the drive cams, the drive roller will translate radially inward as it rotates, thereby breaking contact with the drive shaft drum (at the rotational speeds involved, centrifugal force can be neglected). At the same time, each drive roller guide spring/bearing is being flexed and its return force increased until an equilibrium is reached. Because the translations are so minuscule (in the μ in. region), the forces on the return spring are very small (near preload) and wear and energy loss is minimum.

We will now examine the system which disengages the trailing rollers (CCW drive rollers in the case of CW motor rotation). Figs. 2, 3 and 4 show the drive rollers and lifting magnet system in full scale. Preliminary drawings listed in Appendix: A show the details. From the above Figs., we see that as the drive stroke moves clockwise, each trailing (CCW) roller rolls free of drive deformation and is held in contact with the drive cams and drive shaft drum only by its preload spring. Thus when the lifting magnets above are activated, the striker (star wheel: Fig. 3) preload springs is pulled towards its activated windings in the drive shaft drum. This star wheel impacts each of the trailing rollers on a one by one basis, breaking them loose three at a time until all the trailing rollers are lifted free of contact from their drive cams and the drive shaft drum. It takes considerable current to lift the rollers (2 amps); but

once they are broken loose and the star wheel is in contact with the drive cam with the magnetic flux lines closed, this drops to less than 200 milliamps with power requirements on the order of milliwatts. In this configuration the system acts as a single direction ratcheting device biased towards CW rotation. To reverse direction of rotation we release the CCW drive rollers, activate the lifting magnets above the CW rollers and start ratcheting the motor CCW. The CCW rollers engage the drive shaft drum and drive cams and start to ratchet torque output in a CCW direction. In the first portion of the first stroke of the drive rods, the CW rollers roll free of their drive stroke structural deformations, are lifted by their corresponding magnet and the system acts as CCW-biased ratcheting device.

Figs. 4 show in detail how the lifting system is constructed. The lifting magnet coils are embedded into the drive shaft drum. Above each set of coils is a star wheel which is positioned above its respective coil such that when the coil is activated the magnetic flux attracts the star wheel towards itself with considerable force. This star wheel is held apart from the drive drum by flat springs which are stiff in rotation about Z; but compliant in the Z transverse direction. A disc stand off enables the gap between the star wheel and the drive cam to be set with precision and allows the preload forces in each spring to also be set with precision. Magnet wire (AWG 23) is used and flux lines follow the circuit shown in Fig. 4. A hole is drilled through the center of each drive roller and the roller is fitted over a stainless steel shaft. The shaft is modified to include the addition of radial preload springs (Fig. 9) and the roller is modified to facilitate the addition of a preload spring (Fig.9). Thus, the position of the roller relative to the drive drum cams and drive shaft drum is set along with the forces on those cams and the several compliances (CW, CCW, Z and structural stiffness) of the roller. Also, the coefficients of friction (rotation of the roller about the shaft and sliding up and down on the shaft require a low coefficient of friction and the contact between the roller and the drive drum cams and drive shaft drum requires a high coefficient of friction) are set.

We will now determine whether the magnet can lift the rollers with a sufficient margin of safety. In determining this, we will first determine how high we must lift the roller. We will next determine the forces that must be overcome. Finally, we will examine the power required to lift and hold the roller so that we can see if the solution is practical for extended use.

In determining how high we must lift the rollers we start with the radial errors in manufacturing between the drive cam, the drive rollers and the drive shaft drum. We can assume that these can be held to 0.002 in. These errors

mandate that the rollers be able to ride up and down independently to correct during rotation. We also assume that wear will occur and we allow 0.005 in radial wear. This seems very generous in light of the size of the rollers, their limited rotation and practically nonexistent slip under load and the small number of total rotations the motor must perform (because it is a high torque direct drive device). Since we have a 10 degree cam angle on the drive cam, we have.

$$G_v = \frac{G_r}{2 \tan \psi} \quad \dots(1)$$

Where:

G_v = required lift

G_r = total possible radial gap (manufacturing errors and wear, 0.007in).

ψ = cam angles (10 deg).

We calculate $G_v = 0.006$ in (initial setting) and 0.020 in (after maximum wear). Since our star wheel must lift all rollers some minimum distance to ensure the drive disengagement of each (say 0.005 in.), our gap is 0.025 in. between the star wheel and the drive drum.

We will now determine the forces to be overcome in lifting the rollers. We have the weight of the drive rollers (0.0152 lbs). For reasons that will be explained later in the section on frequency response, we set the radial preload in the direction opposite the direction of drive very light (say 0.25 lbf) and the radial preload in the direction of drive very stiff. Similarly, we set a 0.25 lbf radial preload forcing each roller towards the center of the motor. Thus, our net radial preload inside the hole is 0.35 lbf and the coefficient of friction between these springs and the roller is that of a bearing (say 0.2) with a frictional resistance to lifting of 0.075lbf. We know that the weight of each roller is 0.0152 lbs. And, since we want the rollers to stay in place during the 12 "g" launch environment, we require a vertical preload of

$$12 (0.0152) \text{ lbf} - 0.075 \text{ lbf} = 0.1074 \text{ lbf} \quad \dots(2)$$

this means that the vertical preload spring for each roller is 0.1074 lbf. The star wheel must overcome several forces to include:

- a. 18 vertical preload springs 0.1074 lbf (1.933 lbf).
- b. 18 radial preload frictional forces 0.075 lbf (1.35 lbf).
- c. 18 sets of frictional forces caused by the rollers seating against the drive cams and the drive shaft drum (see Fig.10 and equations shown below) 0.041 lbf (0.489 lbf) for $\mu_s =$

0.3; 0.048 lbf (0.575 lbf) for $\mu_s = 0.5$; 0.0525 lbf (0.944 lbf) for $\mu_s = 0.75$.

During Seating,

$$\Sigma F_z = 0$$

$$F_{pl} - F_{fb} - 2F_{npl} \sin \phi - 2F_{fpls} \cos \phi = 0$$

$$F_{npl} = \frac{F_{pl} - F_{fb}}{2(\sin \phi + \mu_s \cos \phi)} \quad \dots (3)$$

During removal,

$$F_{rz} = F_{pl} - F_{fb} - 2F_{npl} \sin \phi + 2F_{fpl} \cos \phi \quad \dots (4)$$

$$F_{fpl} = \mu_s F_{npl}$$

$$F_{rz} = 2(F_{pl} - F_{fb}) \frac{\mu_s \cos \phi}{\sin \phi + \mu_s \cos \phi} \quad \dots (5)$$

F_{pl} = spring preload force

F_{fb} = Radial bearing frictional force opposing spring preload force

F_{npl} = Normal force caused by seating of bearing

F_{rz} = Resultant frictional force opposing roller removal in z direction

F_{fpls} = Friction force in seating which opposes the preload

F_{fpl} = Friction force after seating which opposes roller removal

ϕ = Roller angle

Adding a., b., and c. together we get the total force required by the star wheel to release all 18 rollers. 3.772 lbf for $\mu_s = 0.3$, 3.858 lbf for $\mu_s = 0.5$ and 4.227 lbf for $\mu_s = 0.75$ (which is extreme). We need a force on the star wheel of 20 lbf at 0.025 in gap to provide a 5:1 safety factor in lifting. This is actually very conservative as we lift the rollers one by one and the air gap will be somewhat less than 0.025 in.

We will now design the electromagnetic lifting mechanism

$$G_v = \frac{G_r}{2 \tan \phi} \quad (\phi = 10^\circ) \quad \dots (6)$$

$$\begin{aligned}
 &= \frac{7.00E-03}{2 \tan 10^\circ} \\
 &= 20 E -03 \text{ inch maximum gap}
 \end{aligned}$$

For initial setting

$$\begin{aligned}
 &\frac{2.0E-03}{2 \tan 10^\circ} \\
 &= 6.0E -03
 \end{aligned}$$

We use tool steel because we want the lifting magnet structure to add to the structural rigidity of the drive drum, to enhance simplicity to reduce the different kinds of metals involved and because our magnetic reluctance path lengths are short compared to the gap so there is little to be gained by going to special magnetic materials. We must overcome 4.227 lbf to lift the 18 rollers in the extreme case.

$$dW_H = FdL = \frac{B_{st}^2}{2\mu_0} SdL \quad [1] \quad \dots (7)$$

Where,

F = force

dL = distance

dW_H = total energy stored in a steady magnetic field

S = core cross sectional area

B_{st} = magnetic flux density in steel

μ₀ = permeability of free space (4πE-7 Henrys/meter)

$$\text{i.e. } F = \frac{B_{st}^2}{2\mu_0} S_{air} \quad [1] \quad \dots (8)$$

B_{st} in saturation is 1.4 Wb/m²

We will use B_{st} = 1.0 Wb/m² to keep below the knee of the B-H curve

$$\begin{aligned}
 \text{i.e. } F &= \frac{B_{st}^2}{2\mu_0} S_{air} \\
 &= 5 \text{ lbs on one gap or } 10 \text{ lbs total} \quad \dots (9)
 \end{aligned}$$

$$\begin{aligned}
 B^2 S_{air} &= 2 (4.448 \text{ N}) (5 \text{ lbf}) 4\pi E-07 \\
 &= 5.589 E-05 \text{ Wb}^2/\text{m}^2 \quad \dots (10)
 \end{aligned}$$

$$\begin{aligned}
 S_{air} &= \frac{\text{plate area}}{2} \\
 &= \frac{\pi((21/16)^2 - (13/32)^2)}{2(39.37)^2} \text{ m}^2 \\
 &= 1.5785 E-03 \text{ m}^2 \quad \dots (11)
 \end{aligned}$$

$$B_{air} = 0.18818 \text{ Wb/m}^2$$

And,

$$\begin{aligned} \Phi &= B_{air} S_{air} \\ &= 2.9704 \text{ E-04 Wb} \\ &= B_{st} S_{st} \end{aligned}$$

$$\text{i.e. } (1.0 \text{ Wb/m}^2) S_{st} = 2.9704 \text{ E-04 Wb}$$

$$\text{i.e. } S_{st} = 2.970 \text{ E-04 m}^2$$

We require 0.125 in thickness in return flange for strength

$$\begin{aligned} S_{st} &= \frac{\pi d_{incoil}(0.125)}{(39.37)^2} \\ &= 2.9707 \text{ E-04 m}^2 \end{aligned}$$

min. $d_{incoil} = 1.172$ in (locates inner diameter of coils.)

Outer diameter $d_{ocoil} = 2.225$ in (and represents the furthest out we can go and still retain structural strength in front of the rollers.)

$$\begin{aligned} r_{ccoil} &= \text{center point (location of slot)} \\ 2\pi(r_{ccoil}^2 - r_{incoil}^2) &= \pi(r_{ocoil}^2 - r_{incoil}^2) \end{aligned}$$

$$r_{ccoil} = \frac{(r_{ocoil}^2 + r_{incoil}^2)}{2}$$

$$r_{ccoil} = 0.97152 \text{ in (as located in Fig. 4)}$$

$$R_{air} = \frac{d_{air}}{\mu_0 S_{air}} \text{ At/Wb}$$

$$d_{air} = 0.02 \text{ in}$$

$$R_{air} = \frac{2(0.025)}{39.37(4\pi \text{ E } -07)1.5785 \text{ E } -03}$$

$$R_{air} = 6.4025 \text{ E } 05 \text{ At/Wb}$$

$$V_m = \Phi R_{air} = 190 \text{ At}$$

We measure the pocket for coils

$$0.5 \text{ in} = d_{ocoil} - d_{incoil}$$

$$0.2 \text{ in high}$$

We use 23 AWG wire, 0.025 in dia with heavy insulation rated at 3.15 ampers.

$$\frac{0.5}{0.025} = 20 \text{ turns per row}$$

$$160 \text{ turns } 0.75 = 120 \text{ turns}$$

$$120 \text{ I} = 190 \text{ At}$$

$$\text{I} = 1.58 \text{ ampers for } 10 \text{ lbf}$$

Since $F \propto B^2$

& $B \propto I$;

we have,

$$F \propto I^2$$

for $I = 2$ amps,

$$F = 10 \left(\frac{2.00}{1.58} \right)^2 \\ = 16 \text{ lbf, using 2 amps}$$

4.2 Torque

In this section we will see if the motor can deliver the large torque expected of it. We will do this by first examining the magnetostrictive drive rods to see if they can deliver the required force. We will then examine the structure, both geometry and materials characteristics, to see if it can sustain the forces of the rods and convert them to torque to the load without major parasitic losses in deformations.

4.2.1 Drive Rods.

The magnetostrictive rods are made of Terfenol-D, Tb₃Dy₇Fe_{1.93} Free Stand Zone Melt (FSZM) and their performance characteristics are shown in Fig.11. We will design the motor for 60 ft-lbs torque. Using the motor configuration shown in preliminary drawings in "Appendix A", we know that we need a force of:

$$F_d = \frac{T_{dr}}{D_{dr}} \quad \dots (12)$$

where:

F_d = rod drive force

T_{dr} = drive torque (60 ft-lbf)

D_{dr} = rod lever arm (1.5 in)

We get a force per rod of 475.17 lbs. This requires using a Terfenol rod of 0.55 in. dia. exerting a force of 2 ksi, which, as we can see from Fig. 11, is well within the state-of-the-art.

We will now explore the structural deflections generated in reaction to the torque. From Fig. 7, we can see that the forces F which are imposed on the drive shaft drum by the drive rollers compress the drive cam along 18 equally spaced radial directions and thus no net compression of the drive cam takes place. (There will be local indentations). The forces N_{cam} act outward on the drive cams. And, since these also are equally spaced, the drive drum is stretched; but (except for local deflections) the drive drum does not deform in an oval pattern. We know:

$$T_{dr} = G * D_{odr} \quad \dots (13)$$

where:

T_{dr} = maximum drive torque (60/40/30 ft-lbs)

G = drive force on drive shaft drum
(213.9/142.59/106.94lbs)

D_{odr} = effective lever arm of output drum (3.3661417 in)

And we know that ψ , the drive cam angle = 10 deg. Thus,

$$N_{cam} = \frac{G}{\sin \psi} \quad \dots (14)$$

$$N_{cam} = 1231.7707/821.18046/615.88535 \text{ lbs for 18 rollers}$$

OR

$$68.431705/45.621137/34.215853 \text{ lbs per roller}$$

4.2.2 Structural Stresses and Strains.

We know that as the motor drives, the drive rollers roll slightly, deform and the drum stretches until the structural reactions balance the torque forces. We desire that this equality of forces occur before the stroke reaches the half way point so that we can get useful motion at maximum torque. At maximum torque, our structural deformations are:

$$Y_r = \frac{p_{dr}}{2Dl^3} * \frac{C_3Ca_2 - C_4Ca_1}{C_{11}} + \frac{M_o}{2D\lambda^2} * \frac{C_{14}}{C_{11}} \quad \dots (15)$$

Where, D and λ are constants which are defined as follow

$$D = \frac{Et_{dr}^3}{12(1.0 - \nu^2)}$$

$$\lambda = \left(\frac{3(1.0 - \nu^2)}{R_{dr}^2 t_{dr}^2} \right)^{0.25}$$

$$C_3 = \sinh(\lambda l_{dr}) \sin(\lambda l_{dr})$$

$$C_4 = \cosh(\lambda l_{dr}) \sin(\lambda l_{dr}) - \sinh(\lambda l_{dr}) \cos(\lambda l_{dr})$$

$$C_{11} = \sinh^2(\lambda l_{dr}) - \sin^2(\lambda l_{dr})$$

$$C_{14} = \sinh^2(\lambda l_{dr}) + \sin^2(\lambda l_{dr})$$

$$Ca_1 = \cosh \lambda (l_{dr} - a) \cos \lambda (l_{dr} - a)$$

$$Ca_2 = \cosh \lambda (l_{dr} - a) \sin \lambda (l_{dr} - a) \\ + \sinh \lambda (l_{dr} - a) \cos \lambda (l_{dr} - a)$$

a = distance from edge of drive drum to location of normal forces on drive drum

y_r = radial deformation of drum
 p_{dr} = total load on drum in lbs per linear inch
 M_o = moment acting on drum in inch lbs per linear inch
 t_{dr} = thickness of drive drum
 R_{dr} = radius of drive drum
 l_{dr} = length of drive drum
 ν = Poisson's ratio
 E = Young's modulus

$$K_{D1} = \frac{D_1 D_2}{D_1 - D_2} \text{ for roller in drive cam}$$

$$K_{D2} = \frac{D_3 D_2}{D_3 + D_2} \text{ for roller on the drive shaft drum}$$

$$b = 2.15 \left(\frac{p_{dr} k_D}{E} \right)^{1/2}$$

$$\Delta r_r = r_r \left(1.0 - \sin\left(\arccos\left(\frac{b}{2r}\right)\right) \right) \dots (16)$$

where,

b = width of rectangular contact area

D_1 = diameter of drive cam

D_2 = diameter of drive roller

D_3 = diameter of drive shaft drum

The total flexure of the structure is the algebraic sum of value given by equation (4) and two values given by equation (5) one each for flexure of drive roller for contact with drive cam and with drive shaft drum respectively and radial flexure of drive cam and drive shaft drum.

The summary of the results are shown in Table 1 to 4:

Table 1: Radial Deformations of Drive Drum

Torque (ft-lbs)	Drum thickness (in)	Deformation (μ -in)
30	0.6125	9.8391435
40	0.6125	13.119165
60	0.6125	19.680127

Table 2: Radial Deformations of Drive Rollers

	<u>Torque (ft-lbs)</u>		
	30	40	60
	<u>Deformations (μ-in)</u>		
1) Roller inside drive cam	14.3231	19.00	28.6477
2) Roller on drive shaft drum	3.15956	4.21275	6.3202

Table 3: Radial Deformations of Drive Cam and Drive Shaft Drum

	<u>Torque (ft-lbs)</u>		
	30	40	60
	<u>Deformations (μ-in)</u>		
a) Drive cam	10.8081	14.4071	21.6158
b) Drive shaft drum	0.035483	0.04658	0.070958

Table 4: Cumulative Radial Structural Deformations

<u>Torque (ft-lbs)</u>	<u>Drum thickness (in)</u>	<u>Deformation (μ-in)</u>
30	0.6125	3.1653870
40	0.6125	50.785595
60	0.6125	76.334793

We calculate that the allowable flexure in a half stroke is 157.1 μ-in. Thus, deformations appear to be manageable. (local deformations remain to be computed using finite element techniques).

The basis of the initial deformation calculations is:

$$\Delta r_{dr} = \frac{R_{dr}}{4} * \Delta L_{dr} * \sin \psi \quad \dots (17)$$

where:

Δr_{dr} = flexure of drum, rollers and drive cam.

(146.52 E-06 in)

R_{dr} = drive ring radius (1.6875 in from scale drawing)

ΔL_{dr} = expansion of drive rods

ψ = angle of drive cam (10 deg)

(The 1/4 factor is because we are using 1/2 stroke and because the rollers roll 1/2 the distance of the stroke)

The contact stresses between drive roller, drive cam and drive shaft drum are shown in Table 5 and can be calculated through following equation.

$$\sigma_{cmax} = 0.591 [E_p c / K_D]^{1/2}$$

Where,

σ_{cmax} = Maximum contact stress

p_c = load in lbs/inch

Table 5: Contact Stresses

Drive Roller Position	Torque (ft-lbs)		
	30	40	60
	Contact Stresses (ksi)		
a. Inside drive cam	27.62	31.89	39.06
b. On drive shaft drum	58.81	67.90	83.16

The elastic limit for high strength alloy steel S.A.E. 52100 is 175-240 Ksi, thus the design is safe.

4.3 Speed/Acceleration/Step Resolution

In this section we will estimate the expected speed, acceleration and step resolution of the motor.

We will begin by first estimating the no load speed requirements of the motor. These requirements determined, we will examine the ability of the motor design to meet these requirements starting with the frequency response of the drive rods. We will then calculate the no load inertial limitations of the device to be allowed by the frequency response of the drive rollers and finally the trailing rollers.

4.3.1 No Load Frequency Response

We will begin by estimating the maximum no load speed. Since this is a direct drive motor with large torque, our rpm can be relatively low and still move the load at reasonably high speeds. For example, 20 rpm at the joint of a 24 in arm will move the tip of that arm at 50 in/s which is excessive for space and fast even by industrial standards. Let us see if we can obtain 20 rpm. Our drive cycle is:

Drive stroke Top/4
 Return Top/4

For a total drive cycle of $T_{op}/2$

Where T_{op} is the period of the operating frequency f (or $T_{op} = 1/f_{op}$).

The angular movement we get per drive stroke is

$$\theta = \frac{\Delta L_{dr}}{r_{rod}} \quad \dots(18)$$

where

ΔL_{dr} = expansion of drive rods

r_{rod} = rod lever arm (1.00 in)

$\theta = 2.0 \text{ E } -03$ radians

To achieve our desired angular speed, we require a steady state operating frequency of.

$$f_{op} = \frac{rpm \cdot p}{60 \cdot \theta} \quad \dots(19)$$

For 20 rpm f calculates to 437 Hz.

The critical frequency f_c for efficient operation of the rods is.

$$f_c = \frac{106.5}{d_t^2} \text{ Hz} \quad [2] \quad \dots(20)$$

where d_t is the Terfenol rod diameter in inches. For our rod diameter of 0.55 in. we get an f_c of 352 Hz. However, if we laminate the rod into four equal segments 0.275 in., we get f_c of 1.4 KHz which is acceptable. Thus rod diameter is not a problem.

No load inertial limitations involve the rods, the drive drum and the drive and trailing rollers. We can neglect the output drum and output drive shaft because they store kinetic energy in the no load condition.

The frequency response of motor under no load depends on the inertia of oscillating parts of motor. The inertia of oscillating parts, torque and angular acceleration of motor are related by the following well known equation:

$$T_{dr} = \Sigma J_{osc} \alpha_{nl} \quad \dots(21)$$

Where,

ΣJ_{osc} = Polar Moment of Inertia of Oscillating Members of Motor (lb ft sec²)

T_{dr} = Torque (60 ft lbf)

α_{n1} = No Load Angular Acceleration of Motor
(rad/sec²)

The individual polar moment of inertias calculated from the data taken from preliminary drawings listed in "Appendix A" is shown in following table.

Table 6: Polar Moment of Inertia (J_{osc}) of Oscillating Members

J_{osc} (ft lb sec ²)			
Member	Each	No/Stage	Total
Rollers	7.4238E-06	36	2.67256E-04
Preload Plates	0.0137712	2	0.0275424
Drive Drum	0.1263266	1	0.1263266

$$\Sigma J_{osc} = 0.1541362$$

Substituting the values of ΣJ_{osc} and T_{dr} in equation (21), we get
 $\alpha_{n1} = (389.26/259.51065/194.63299)$ rad/sec² for 60/40/30 ft-lbs torque.

The angular movement θ , angular acceleration α_{n1} and time T_{n1} are related by following equation:

$$\theta = 0.5 \alpha_{n1} T_{n1}^2 \quad \dots (22)$$

Where,

$$\theta = 2.0 \text{ E } -3 \text{ rad}$$

From equation (22) we have,

$$T_{n1} = (3.20558 \text{ E } -03/3.9260 \text{ E } -03/4.53337 \text{ E } -03) \text{ seconds}$$

The no load frequency of the motor can now be calculated by the following relationship,

$$f_{n1} = 1/2T_{n1}$$

$$= 155.97799/127.35549/110.29309 \text{ Hz}$$

4.3.2 On Load Frequency Response

The individual polar moment of inertias of moving masses calculated from the data taken from the preliminary drawings listed in "Appendix A" is as shown in the following table.

Table 7: Polar Moment of Inertia (J_{rot}) of Rotating Members

J_{rot} (ft lb sec ²)	
Member	Single Stage
Drive Shaft Drum	0.0896217
Shaft	3.17753 E -04

$$\Sigma J_{rot} = 0.0899394$$

Table 8: Polar Moment of Inertia (J) Oscillating and Rotating Members

Member	J (ft lb sec ²) Single Stage
Oscillating	0.1541362
Rotary	0.0899394

$$\Sigma J = 0.2440756$$

Substituting the values of ΣJ and T_{dr} in equation (21), we can compute values of on load angular acceleration α_{o1} , time T_{o1} and frequency f_{o1} . The results are as shown in the Table 9.

Table 9: On Load Angular Accelerations and Frequency Response

Torque	Single Stage		
	Acceleration α_{o1} (rad/sec ²)	time T_{n1} (seconds)	Frequency f_{o1} (Hz)
60.00	245.82547	4.03382 E-3	123.95199
40.00	163.88365	4.94042 E-3	101.20636
30.00	122.91274	5.70468 E-3	87.647335

We will now show how high speed operations affect the rollers being held by their lifting magnets.

4.4 Temperature

Part of the input power to the various coils is converted to heat due to hysteresis and eddy current losses. In addition to this, heat contributed by friction in roller locking mechanism also tends to increase to temperature of the motor. The heat generated produces a temperature rise which must be controlled to prevent damage to or failure of the windings by breakdown of the insulation at elevated temperatures. This heat is dissipated from the exposed

surfaces of the motor by a combination of radiation and convection. The dissipation is therefore dependent upon the total exposed surface area of the core and windings.

4.4.1 Coil Losses

Coil losses can be broken down into two components;

1. Core loss which is fixed loss and,
2. Copper loss or Quadratic loss, which is a variable loss and is related to the current demand of the load. The coils are most efficient when core losses and copper losses are equal. In all further calculations, for simplicity, we will presume that this condition is valid for all the coils, viz., for electromagnets as well as for the Terfenol rod driving coils. We will now proceed to estimate the coil losses for electromagnets as well as for the Terfenol drive rods.

Electromagnet Coil

The specifications of the electromagnet coil is as follow:

Table 10: Electromagnet Coil Specifications

AWG	I.D.(in.)	O.D.(in.)	Length(in.)	No. of Turns	I(amp)
23	1.7	2.2	0.24	120	2.0

The specifications of the coil wire is as follow:

Table 11: Coil Wire Specifications

Size (AWG)	Dia(in.)	DC Resistance at 20° C Ohms/1000 Ft
23	0.025	21.1

The total length of the wire can be estimated to be 24.504423 feet. The DC resistance of this wire from the data from the above table is 0.5170433 Ω . The copper loss (and in tern heat) is proportional to the square of the current and resistance of the coil. That is,

$$\begin{aligned}
 H_{cu1} &= I_1^2 R_{coil1} && \dots (23) \\
 &= 0.2^2 * 0.5170433 \\
 &= 0.020681733 \text{ Watts}
 \end{aligned}$$

From our earlier assumption, Core loss, $H_{co1} = H_{cu1}$. Thus total loss in electromagnet coil is 0.041363466 Watts.

Terfenol Rod Coil

The specifications of the Terfenol rod coil is as follow:

Table 12: Terfenol Rod Coil Specifications

AWG	I.D.(in.)	O.D.(in.)	Length(in.)	No. of Turns	I(amp)
23	0.55	1.2	1.75	1016	2.0

The specifications of the coil wire is as in Table 11. The total length of the wire can be estimated to be 209 feet. The DC resistance of this wire from the data from the above table is 4.4499 Ω. As earlier the copper loss is,

$$\begin{aligned}
 H_{Cu2} &= I^2 R_{coil2} \\
 &= 2^2 * 4.4499 \\
 &= 17.6396 \text{ Watts}
 \end{aligned}$$

Since H_{Co2} (Core loss) = H_{Cu2} . Thus total loss in Terfenol rod coil is 35.2792 Watts.

The losses incurred in the above discussed coils is as tabulated in Table 13.

Table 13: Heat losses in coils

1. Electromagnet Coil			
Losses	No.	Watts/each	Total
Copper Loss	2	0.020681733	0.041363466
Core Loss	2	0.020681733	0.041363466
2. Terfenol Rod Coil			
Losses	No.	Watts/each	Total
Copper Loss	4	17.6396	70.5584
Core Loss	4	17.6396	70.5584

$$\Sigma \text{Loss} = 141.19953 \text{ Watts}$$

4.5 Designing For Wear

Since the wear of various components of roller drive affect the performance and the replacements of these components are impractical, wear and wear predictions are of major concern. There are a large number of variables which affect wear. Structural properties of the material, hardness, state of lubrication, load/pressure, sliding velocity, sliding time, surface temperature rise, size, finish, clearance and ambient temperature are the various parameters which affect wear. The most important and independent ones are the load and the velocity as these are dictated by the system requirements. The sliding distance is determined by the velocity and sliding time or duty cycle. Two extremely important dependent variables are the surface temperature rise due to frictional heating and the state of the lubrication in the various interfaces. Changes in the values of these variables will bring changes in the wear rate

in any given application; however, even more significantly, there are critical values of these operating variables where there will be large increases (or decreases) in the wear rate. The graphs of Fig. 11 shows how the wear rate changes. The wear rate is defined as the rate of change of the wear volume, W_r is determined as:

$$W_r = \frac{W_2 - W_1}{t_2 - t_1} \frac{\text{cm}^3}{\text{sec}}$$

where,

- t_1 = time of first observation
- t_2 = time of second observation
- W_r = rate of wear
- W_1 = wear at time t_1
- W_2 = wear at time t_2

4.5.1 EFFECT OF DESIGN VARIABLES

1. Time

Fig. 11(a) shows the effect of the time on wear. After initial "run in" which occurs at a high wear rate, the wear rate decreases to a constant value. The wear rate differs for different conditions of lubrication. The wear rate for a boundary lubricated bearing can be 10^5 times that for a fluid lubricated bearing. An unlubricated bearing can have a wear rate 10^5 times that for boundary lubrication.

2. Load

The wear rate increases as the load increases in an unlubricated bearing. This increase in wear rate is due to the increase in temperature which soften the material or it will be due to breakdown of the surface films, usually oxides, which have prevented surface damage and wear.

3. Velocity

Wear rate in unlubricated contact usually increases with increase in velocity due to thermal softening of the material.

4. Temperature:

Constant wear rate are observed in unlubricated contacts until the material softens appreciably. Increase in temperature can have the following effects:

- Increase in wear rate
- rate of wear increases as the rate of oxide film formation increases with temperature.
- Breakup of oxide films at higher temperatures enhances adhesive wear.
- All forms of chemical wear are increased.

4.5.2 EFFECTIVE WEAR CONTROL

Roller drive functions efficiently if the friction between contact surfaces is maximum. This demands that those contacts be maintained unlubricated at all the times. As such the relevant design factors for this applications are proper material selection, surface finish, temperature control and motion control. Of these parameters, motion control variables are set by system requirements.

1. Material Selection

The secondary requirements (strength, fatigue resistance, relative thermal expansion, dimensional stability, ease of fabrication and cost etc.) make material selection the most important step in wear control. Three methods are available to select material for wear resistance:

a. Known properties (non welding, low ductility, high hardness, limited slip, adhesion preventing films, higher friction, high carbon content, increased work hardening, higher toughness, higher tensile strength etc.) which control wear.

b. Identify similar applications under similar operating conditions and select same materials.

c. Use of material priority tables for a given type of wear.

Existing technical literature corresponds to the category 'c'.

2. Surface Finish

When soft material slide against harder material, hard material can cut or abrade the softer.

3. Temperature Control

Whenever, temperature exceeds beyond certain limits, consideration should be given to,

- Additional air flow around the components
- Improved flow path from the surface
- Reduced load or sliding velocity
- Using materials with better heat dissipation qualities (higher conductivity, higher densities and higher specific heat).

4.5.3 WEAR PREDICTION TECHNIQUE

Amount of wear over a certain time period can be estimated by three techniques.

1. Analytical

Here a simple wear equation is proposed and attempts are made to account for significant variables, either directly or through wear coefficients.

2. Component

Here wear is measured under controlled conditions in component test or prototype test. These results are then extrapolated to service usage.

3. Service Wear Measurements

Here wear is measured either directly or indirectly on components in service or those temporarily removed from service. Wear of similar components in the same application is predicted using the resulting wear/time behaviour. The results may be based on a few measurements at a single point in time or statistically correct wear time distributions to which probability theory is applied. In our discussion we will concentrate only on analytical technique to estimate wear or life of various components of roller drive.

4.5.4 ANALYTICAL TECHNIQUE

From a functional point of view, wear is seen to be represented as follows:

$$W = f(\alpha_{en}, \beta, \frac{K_m \phi_f}{H}, j, L, V, T, t) \quad \dots (24)$$

Where,

- W = Wear
- α_{en} = Environmental effects
- b = Geometric effects
- K_m = Wear coefficient
- ϕ_f = Finish factor
- H = Hardness
- j = Film thickness
- L = Load
- V = Velocity
- T = Temperature
- t = Time

From component or laboratory tests, the functional equation can be reduced to:

$$W = \frac{K_m L V t}{H} \quad \dots (25)$$

$$= \frac{K_m L d}{H} \quad \dots (26)$$

Where,

- W = Volumetric wear
- K_m = Dimensionless wear coefficient

Since,

$$W = Ah; P = \frac{L}{A}$$

$$h = \frac{K_m P V t}{H} = \frac{K_m P d}{H} \quad \dots (27)$$

Where,

h = wear depth perpendicular to the contact area
 d = sliding distance
 A = Contact area (apparent)
 P = Contact pressure
 H = Hardness
 L = Load
 V = Velocity
 t = time

In equation (27) the dimensionless K_m includes all of the factors of Eq. (27) not explicitly given; that is α_{en} , β , ϕ_f , T and j. K_m is determined from the wear/time curve:

$$K_m = \frac{(W_2 - W_1) H}{(t_2 - t_1) L V}$$

$$\text{or} = \frac{(h_2 - h_1) H}{(t_2 - t_1) P V}$$

For surfaces which are not continuously in contact (e.g., rolling contacts) Fein [3] has developed the following equations derived from and equivalent to equation (24).

$$h_2 = \frac{K_m}{H} \frac{L n}{P} \frac{|U_s|}{U} \quad (\text{Load Equation}) \quad \dots (28)$$

$$h_2 = \frac{K_m}{H} P_{nc} \frac{|U_s|}{U} \quad (\text{Pressure Equation}) \quad \dots (29)$$

Where,

h_2 = Depth of wear at center of worn area
 c = Width of load support in rolling direction
 H = Dimensionless wear coefficient
 n = Number of times surface passes through Loaded area
 P = mean pressure
 U_s = sliding velocity (i.e. vector difference between the rolling velocities of two surfaces at load area)
 U = Rolling Velocity (i.e. sweep velocity of the wearing surface through the loaded area)
 L = Load

The hardness values inserted in Eqns (24, 29) are those for the surface being measured or the wearing surface. Where both surfaces are wearing, the total wear is the sum of the wear of each surface calculated independently:

$$h_t = h_1 + h_2$$

Where,

h_1 = Depth of wear on body 1
 h_2 = Depth of wear on body 2

4.5.5 WEAR CALCULATIONS FOR DRIVE CAM

Considering the small area on cam on which the drive roller is constrained to roll and slide repeatedly, drive cam forms the basis of wear design calculations. All other surfaces i.e. drive roller and drive shaft drum due to their larger diameters and hence larger surface area, then will be much safer if the wear design is based on cam wear calculations.

Selecting bearing material 52100 steel for drive cam with hardness of 653 DPH/Rc 58 and Wear coefficient of $1.1 \text{ E-}5$ for dry contact, we have from equation (29);

$$n = \frac{h H}{K_m P c \frac{|Us|}{U}} \quad \dots (30)$$

where,

$$H = 9.3852 \text{ psi}$$

$$K_m = 1.1 \text{ E-}5$$

$$P = 39.06 \text{ E}3 \text{ psi}$$

$$\frac{|Us|}{U} = 1.40452 \text{ E-}3$$

$$c = 1.12515 \text{ E-}3$$

$$h = 0.007 \text{ inch}$$

Substituting the above values in Equation (30) we get, $n = 1.62117 \text{ E}9$. This evaluates to life of drive cam of 636(785) Hours at 20 R.P.M.

4.6 CLOSURE

Considering the intermittent operation of the motor required to screw and unscrew bolts and other duties required in space, the wear life of 636 Hrs at 20 R.P.M. is adequate. Thus the roller drive will theoretically run at 20 R.P.M. for 636 hours without any appreciable deterioration in performance of the motor.

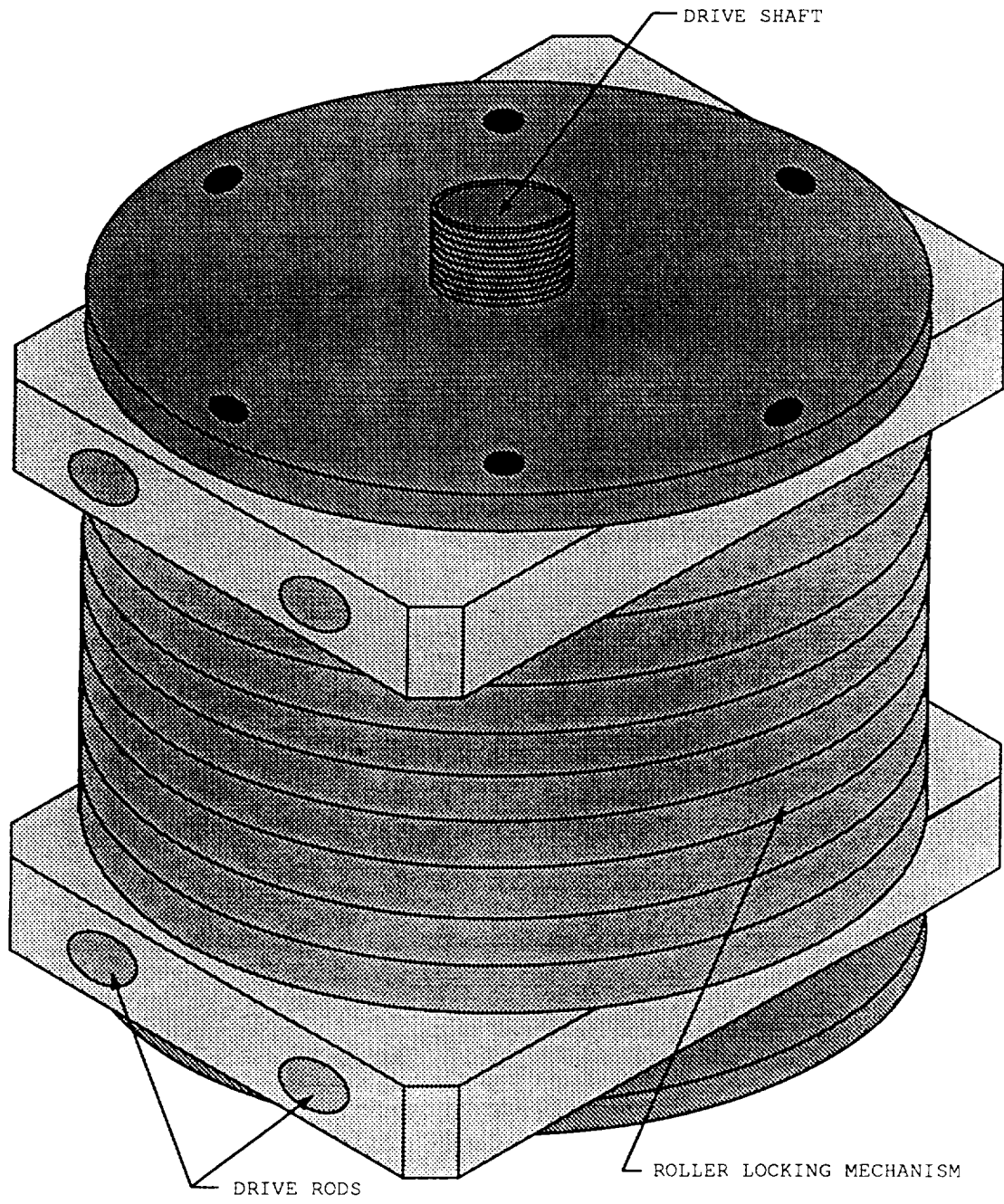


Fig. 1 Magnetostrictive Direct Drive Motor

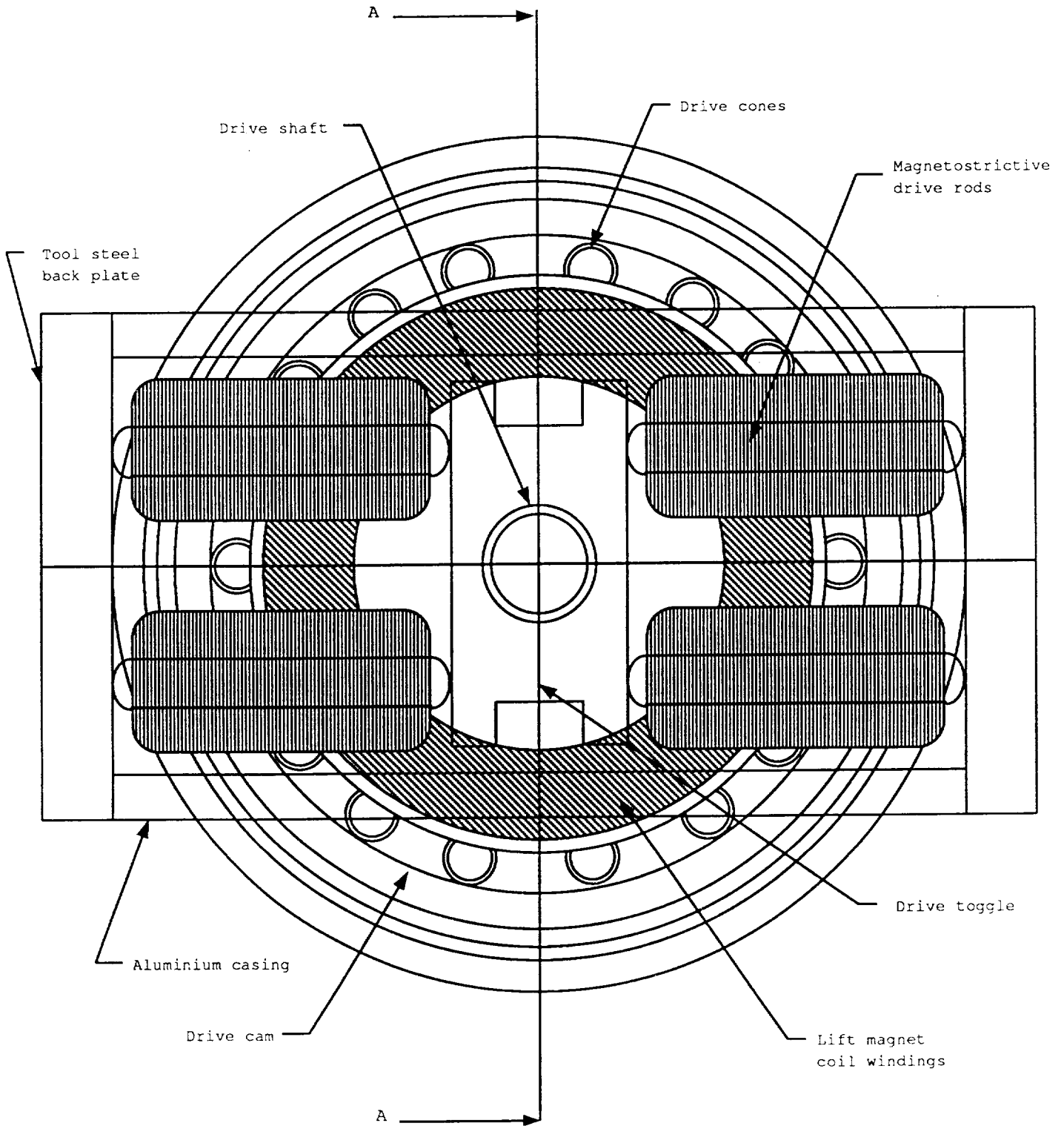
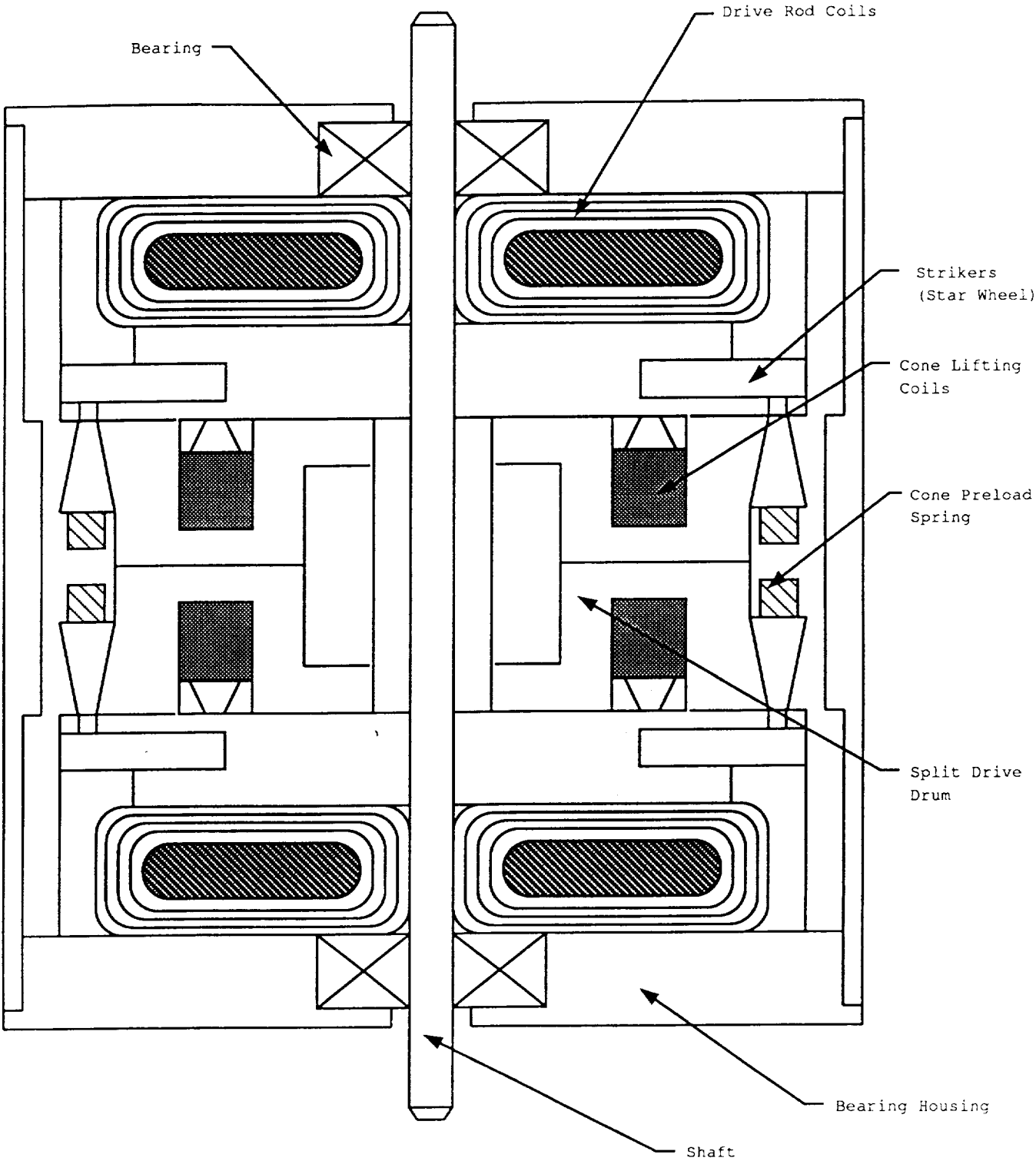


FIG. 2 TOP VIEW OF MOTOR



Section A - A

Fig. 3 Front View of Motor

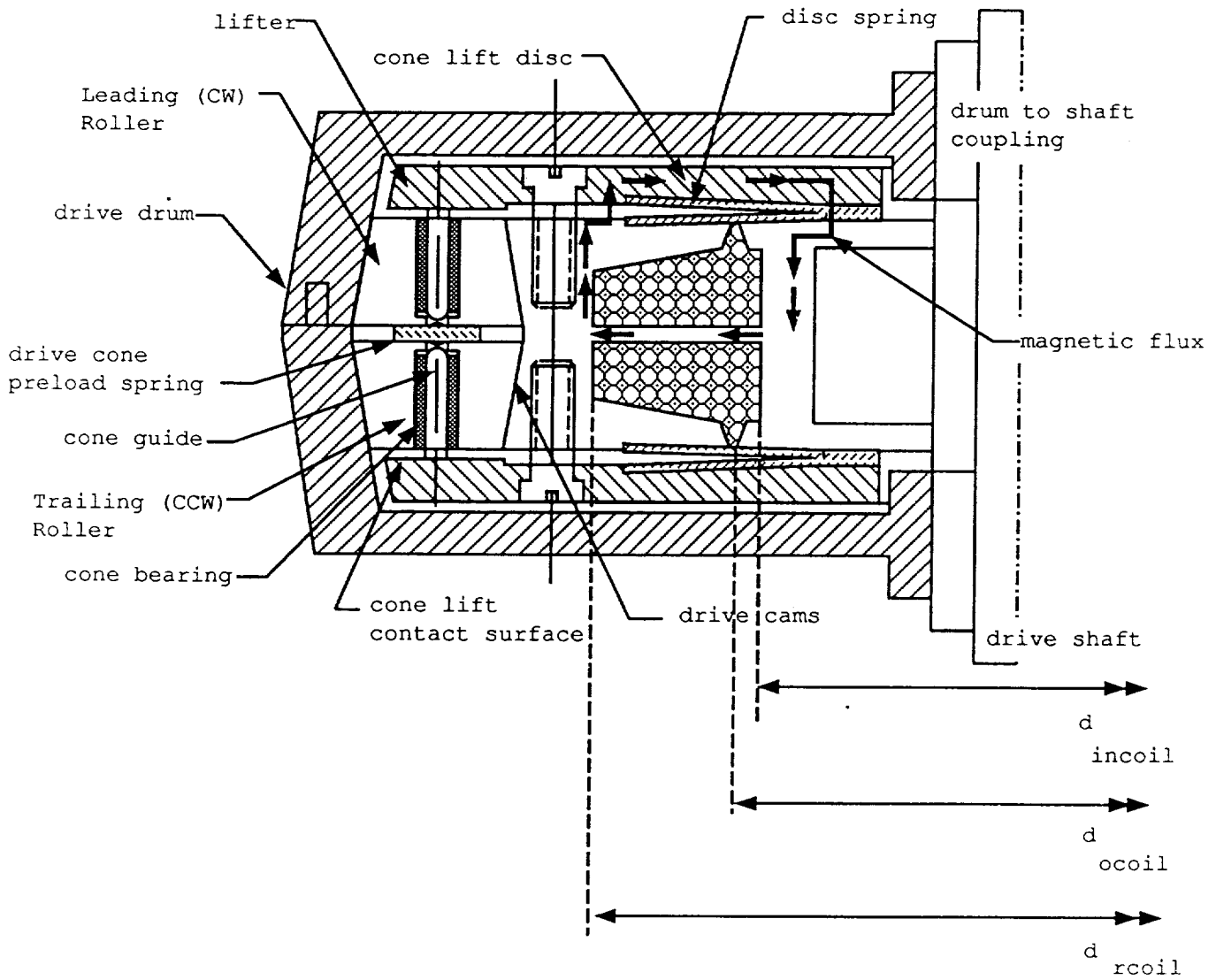
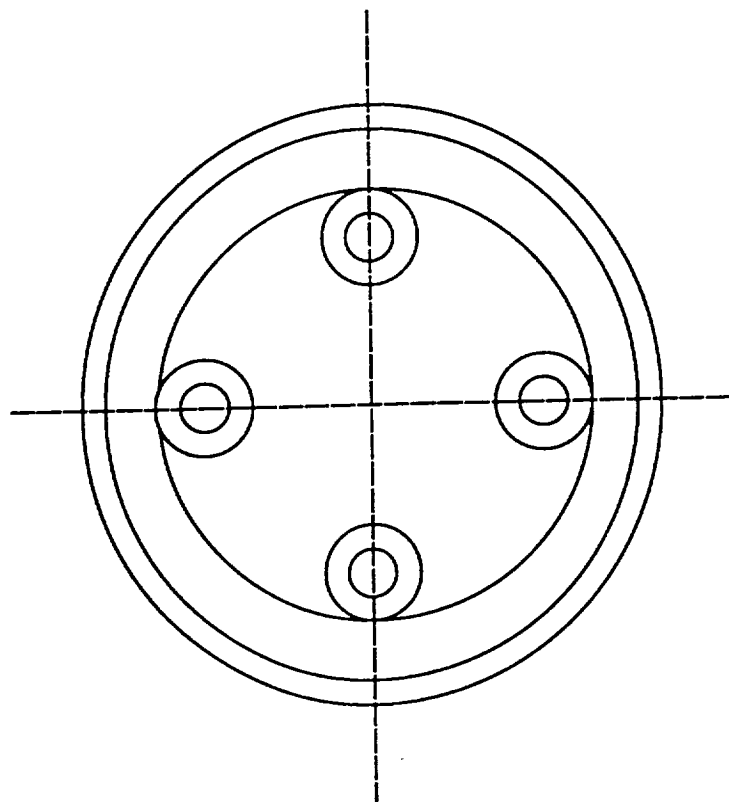
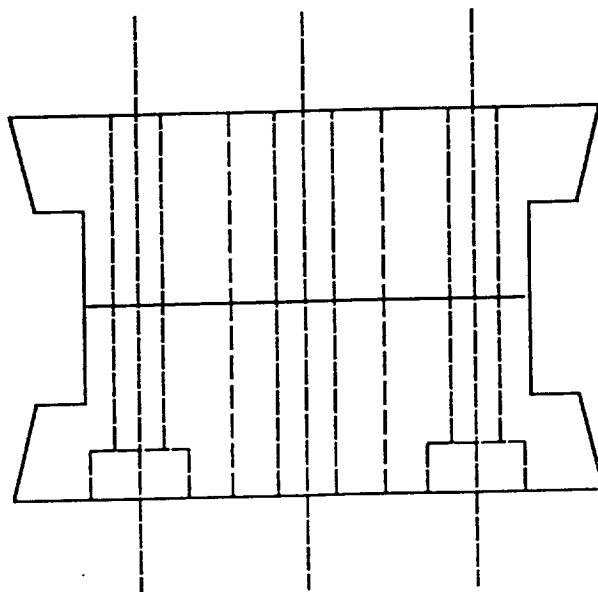


Fig. 4 Locking Roller Drive Details



PLAN



ELEVATION

Fig. 5 Drive Shaft Drum

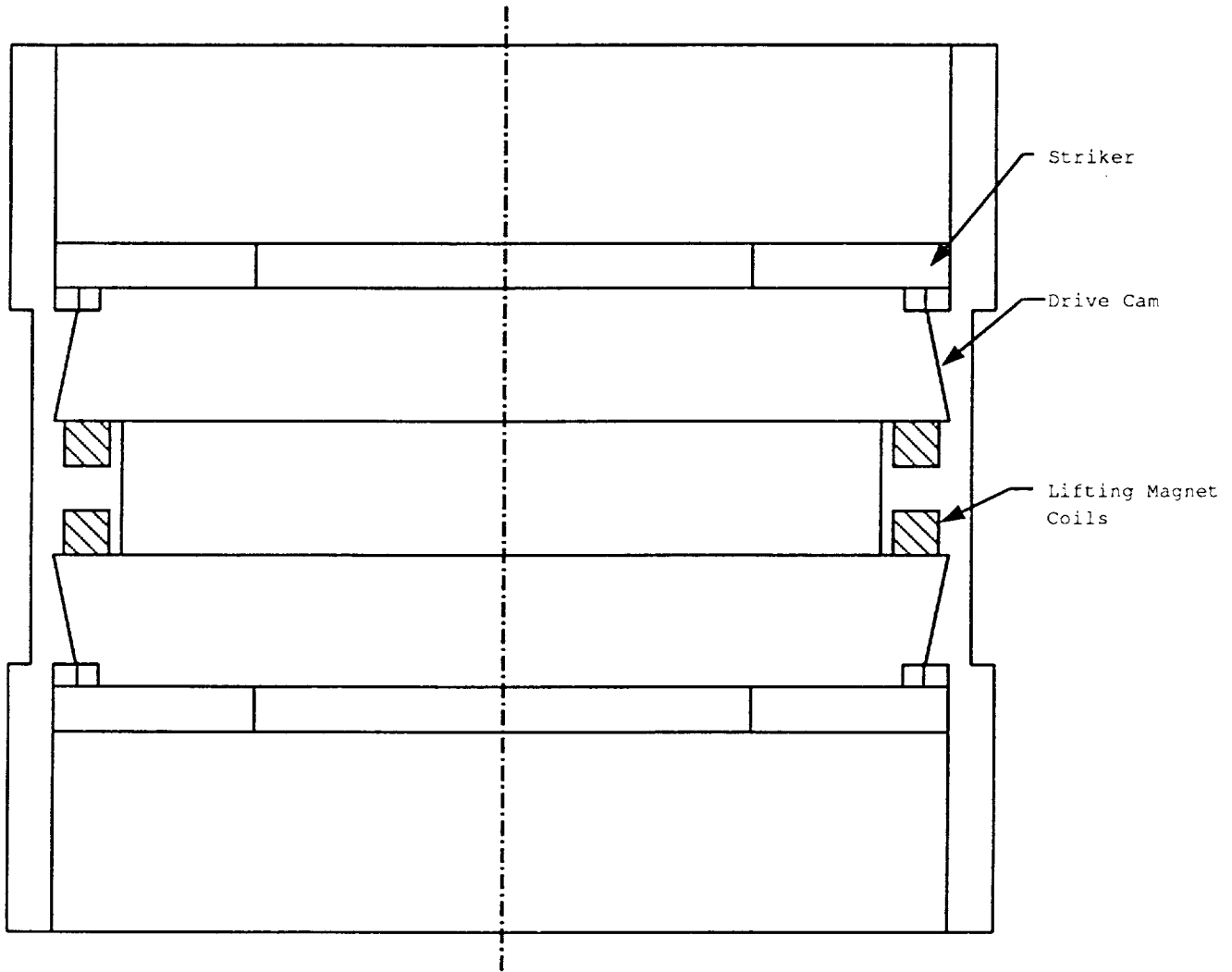


Fig. 6 Drive Drum

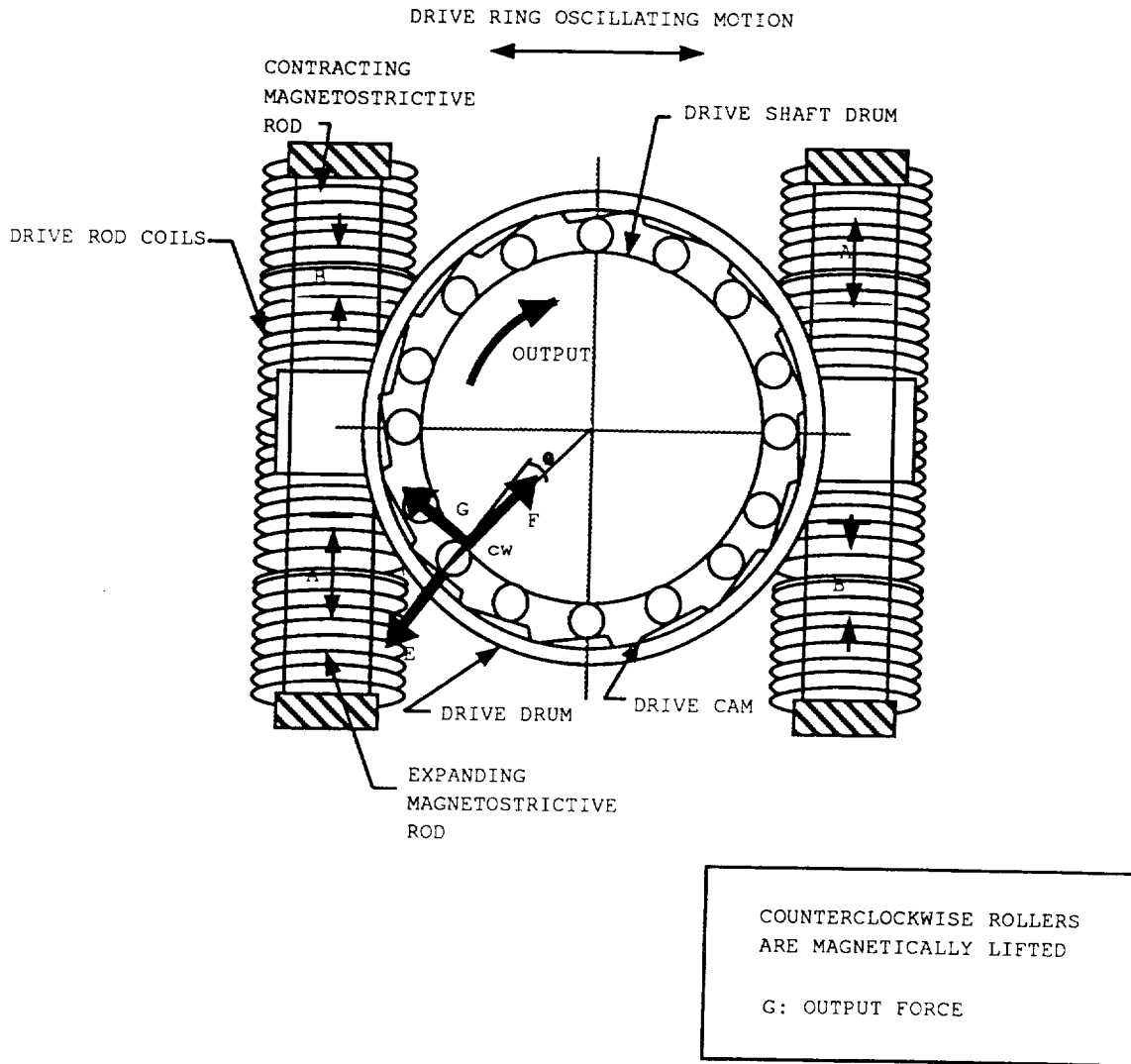


FIG. 7 FUNCTIONAL OPERATION OF DRIVE

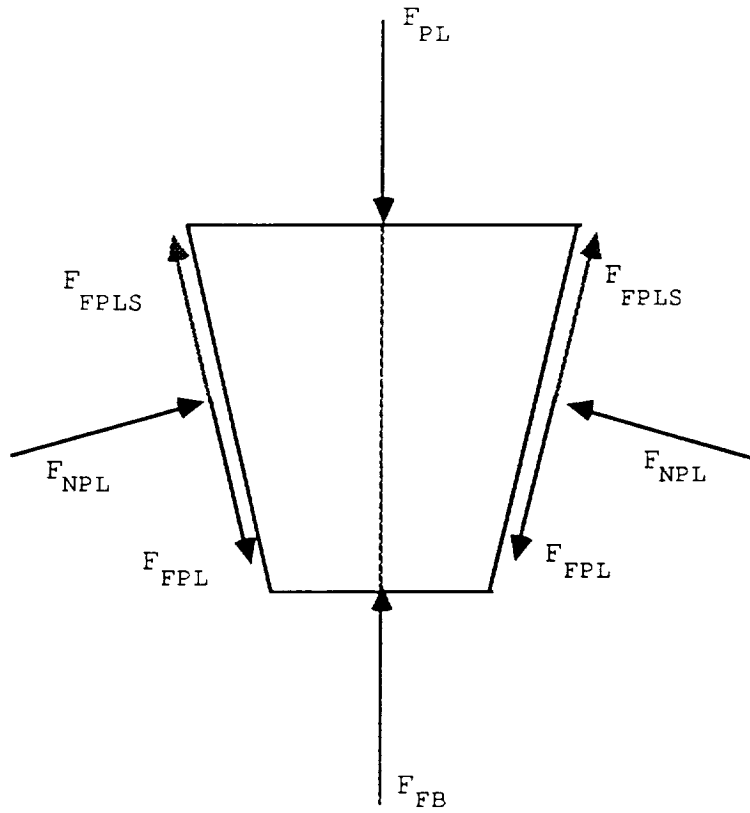


FIG. 8 (a) PRELOAD FORCES

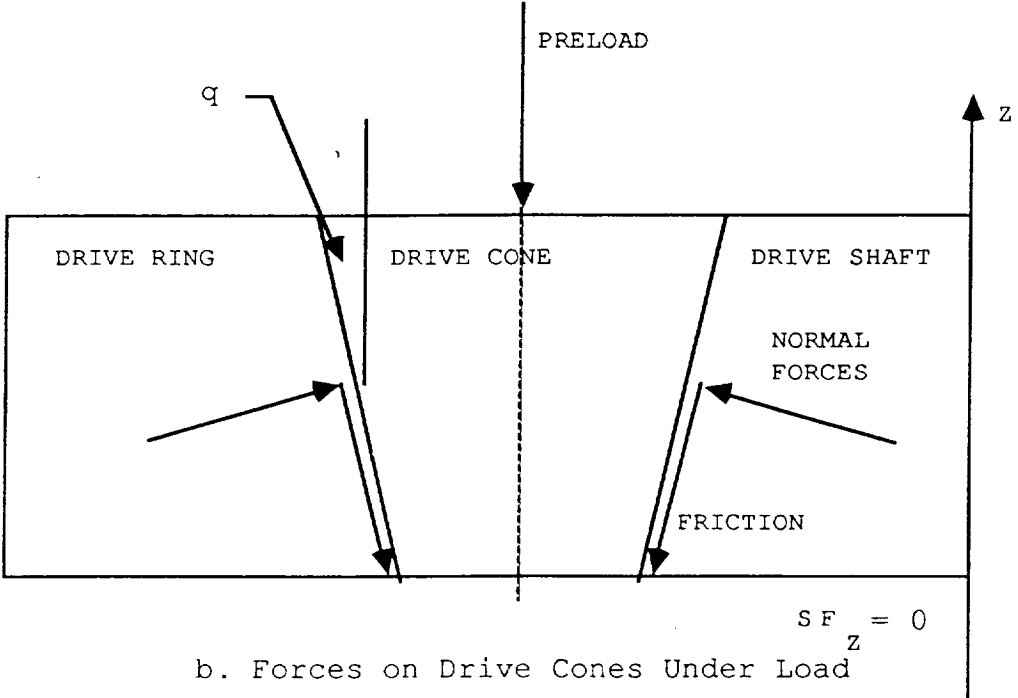
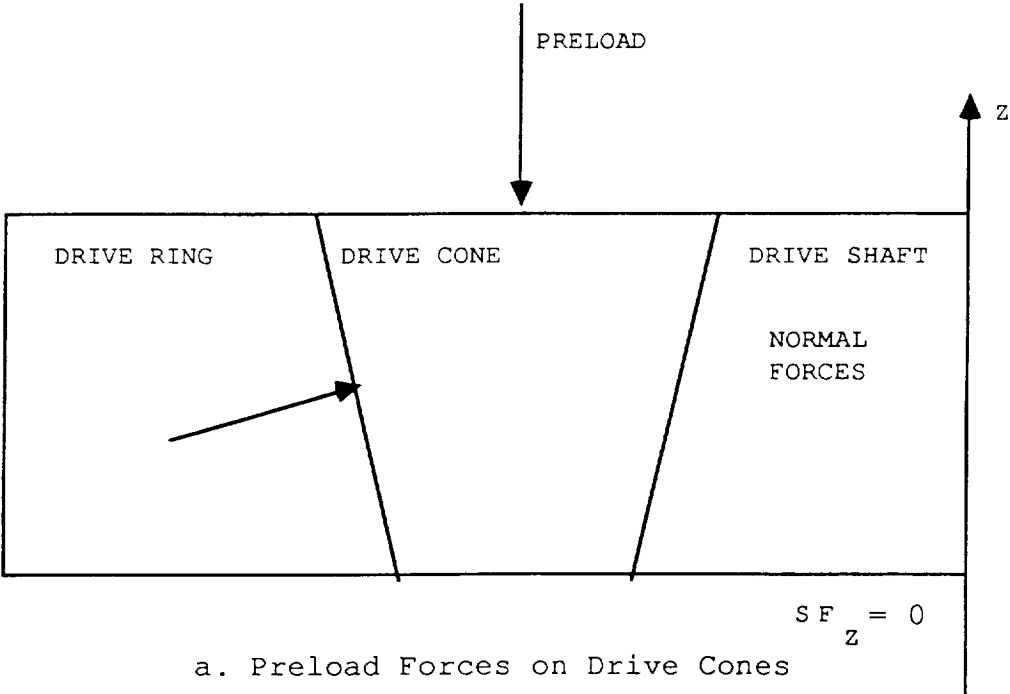


FIG. 8 (b) PRELOAD FORCES

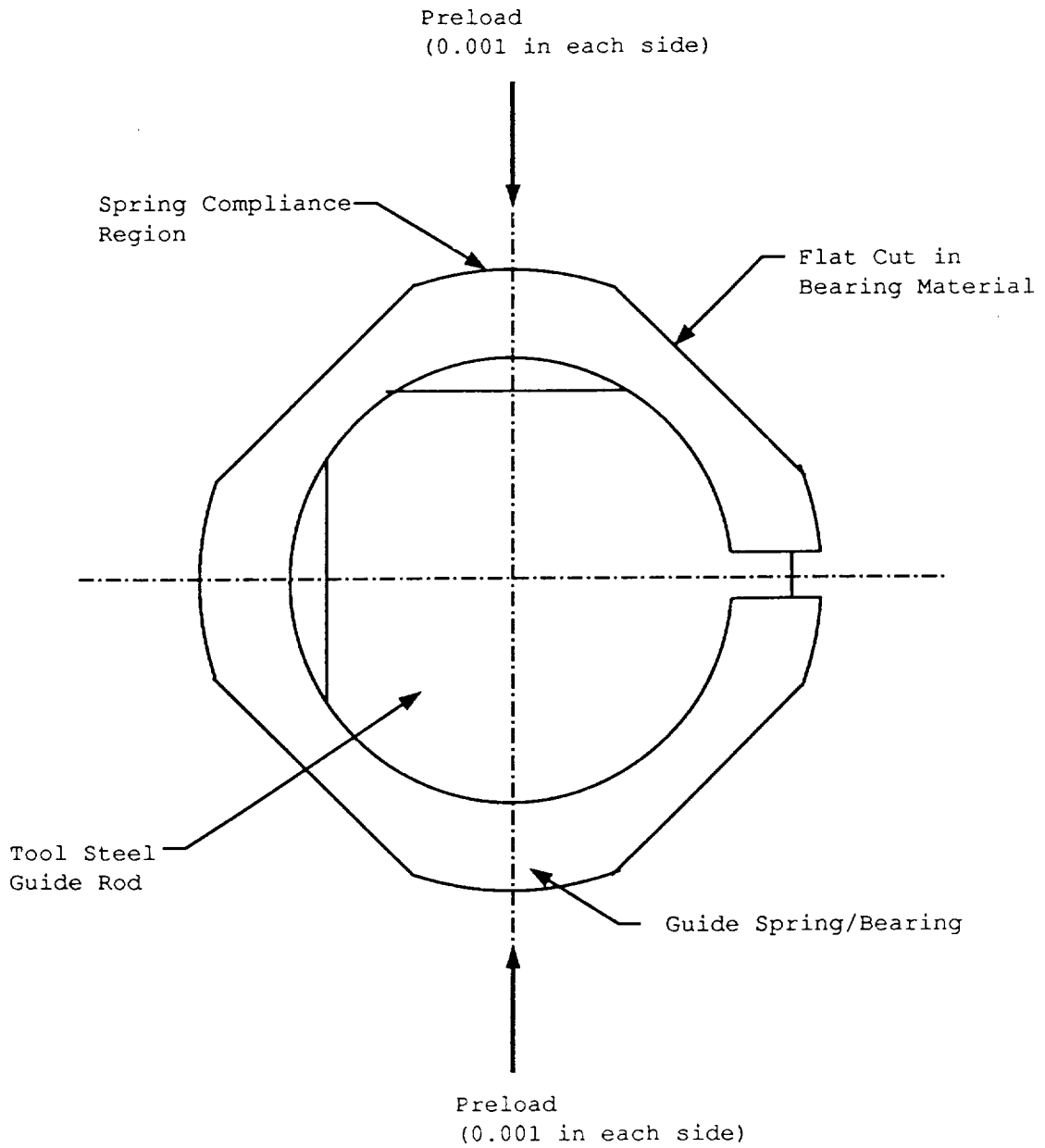
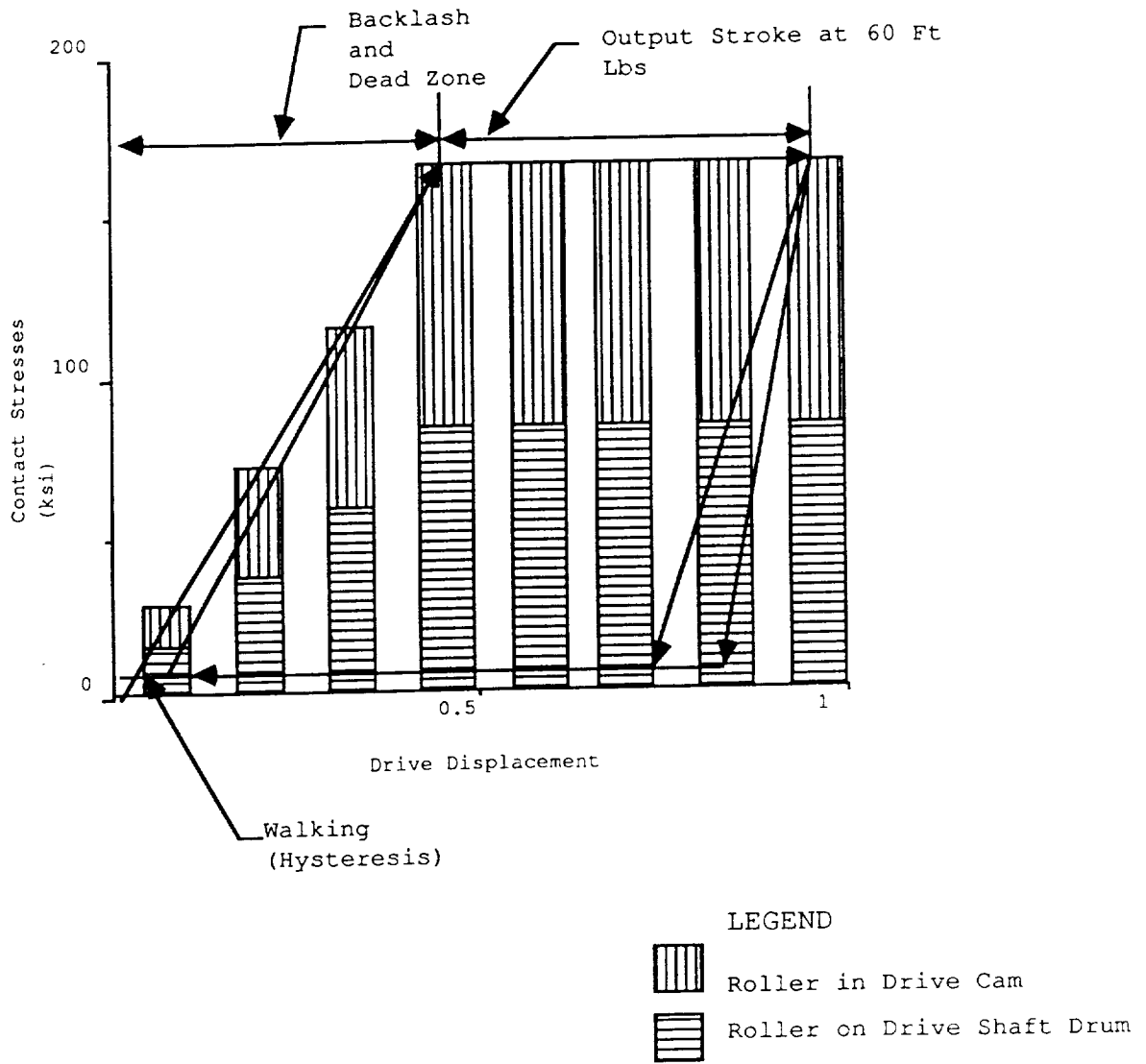


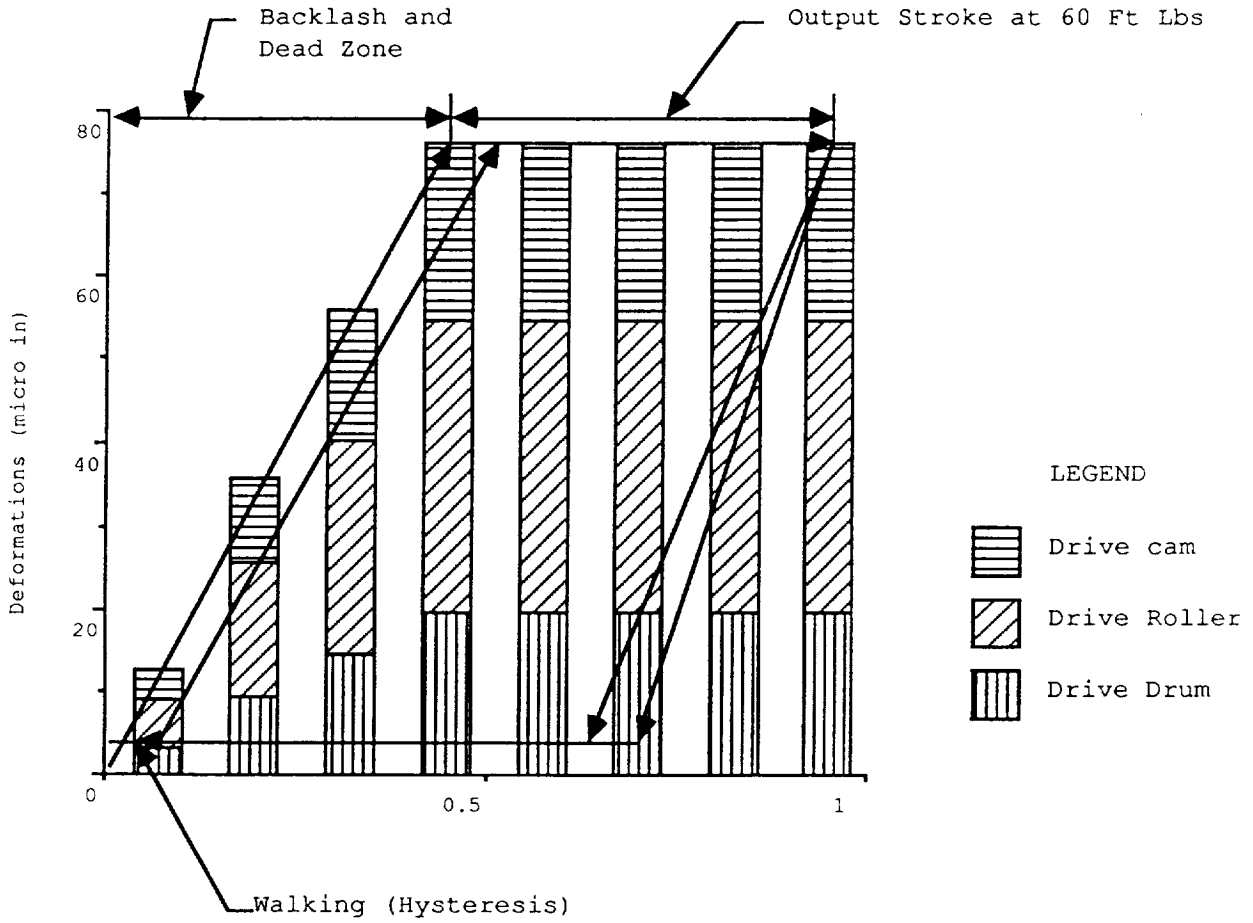
Fig. 9 Guide Spring



(a)

CONTACT STRESSES

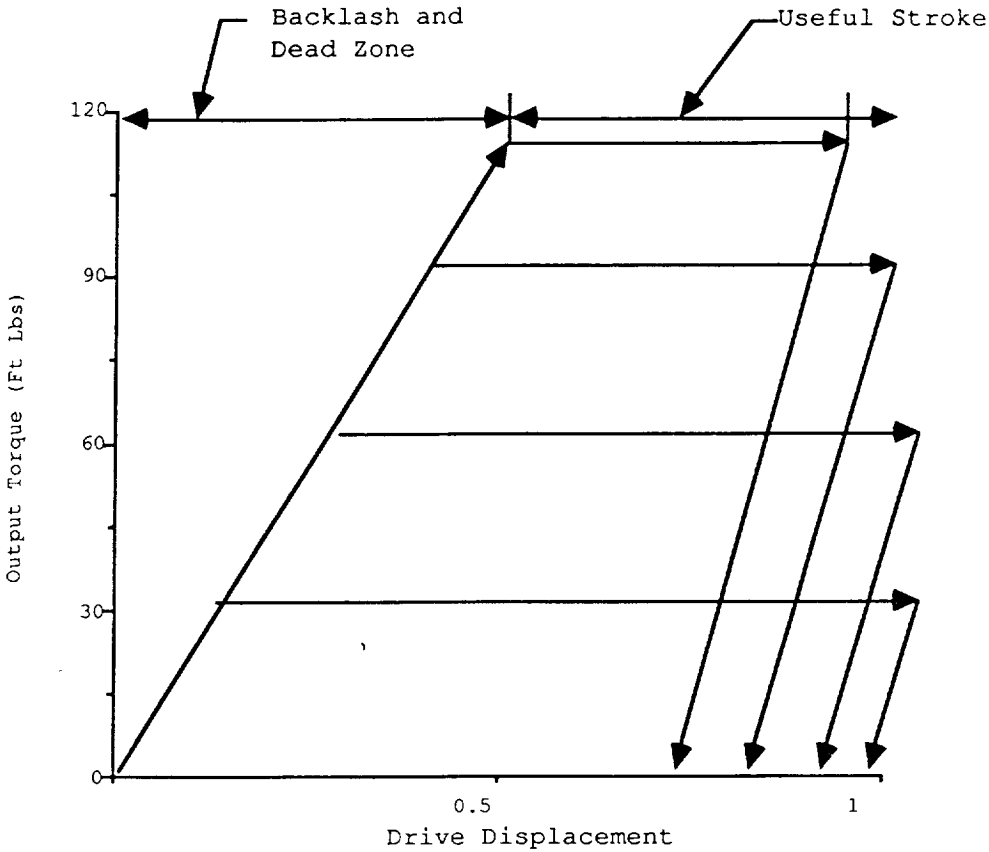
Fig. 10 Regions of Backlash, Dead Zones and Hysteresis



(b)

DEFORMATIONS

Fig. 10 Regions of Backlash, Dead Zones and Hysteresis



(c)

Steady State Torque Output

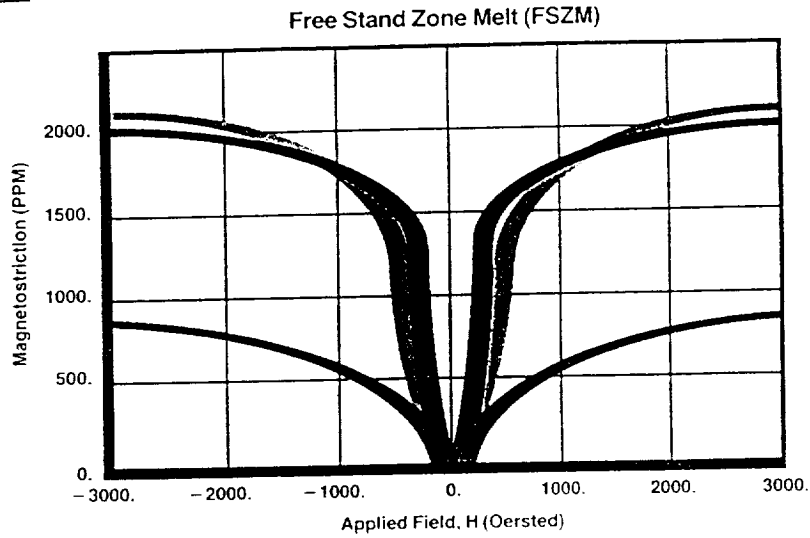
Fig. 10 Regions of Backlash, Dead Zones and Hysteresis

ETREMA TERFENOL-D MAGNETOSTRICTION

Highest performance material
 $Tb_{0.7}Dy_{0.3}Fe_{1.93}$
 directionally solidified
 (FSZM) near single crystal -
 6.3mm (.25 in.) diameter

PRESTRESS

- 2.0 KSI
- 1.0 KSI
- 0.0 KSI



Typical performance of
 $Tb_{0.7}Dy_{0.3}Fe_{1.93}$
 directionally solidified (MB)
 material - 10mm
 (.4 in.) diameter

PRESTRESS

- 2.0 KSI
- 1.0 KSI
- 0.0 KSI

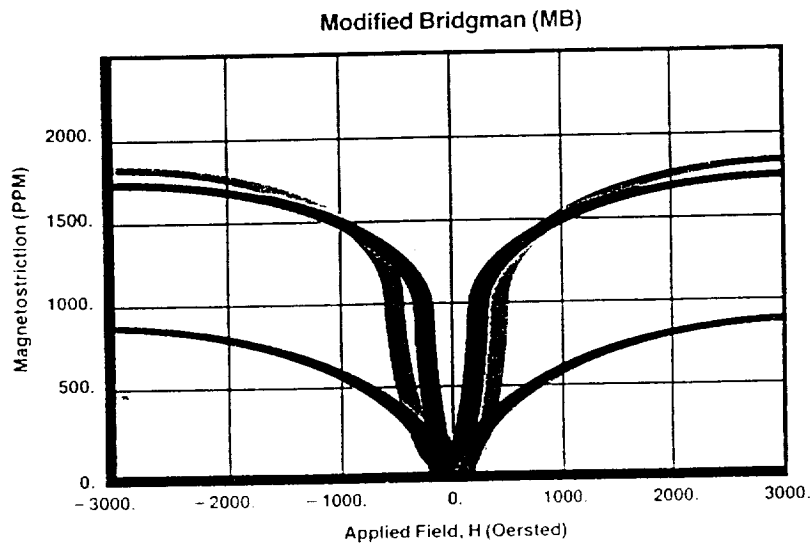


Fig. 11 Performance Characteristics of FSZM Terfenol Rods

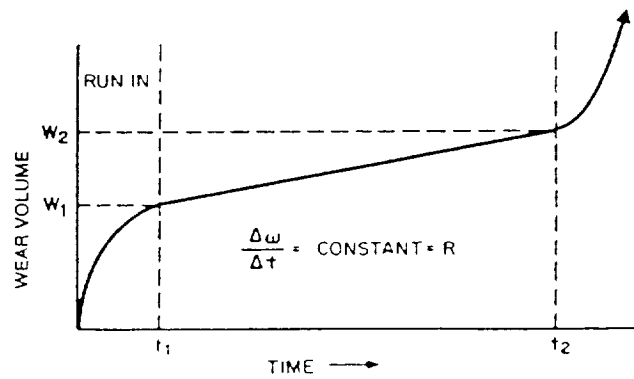
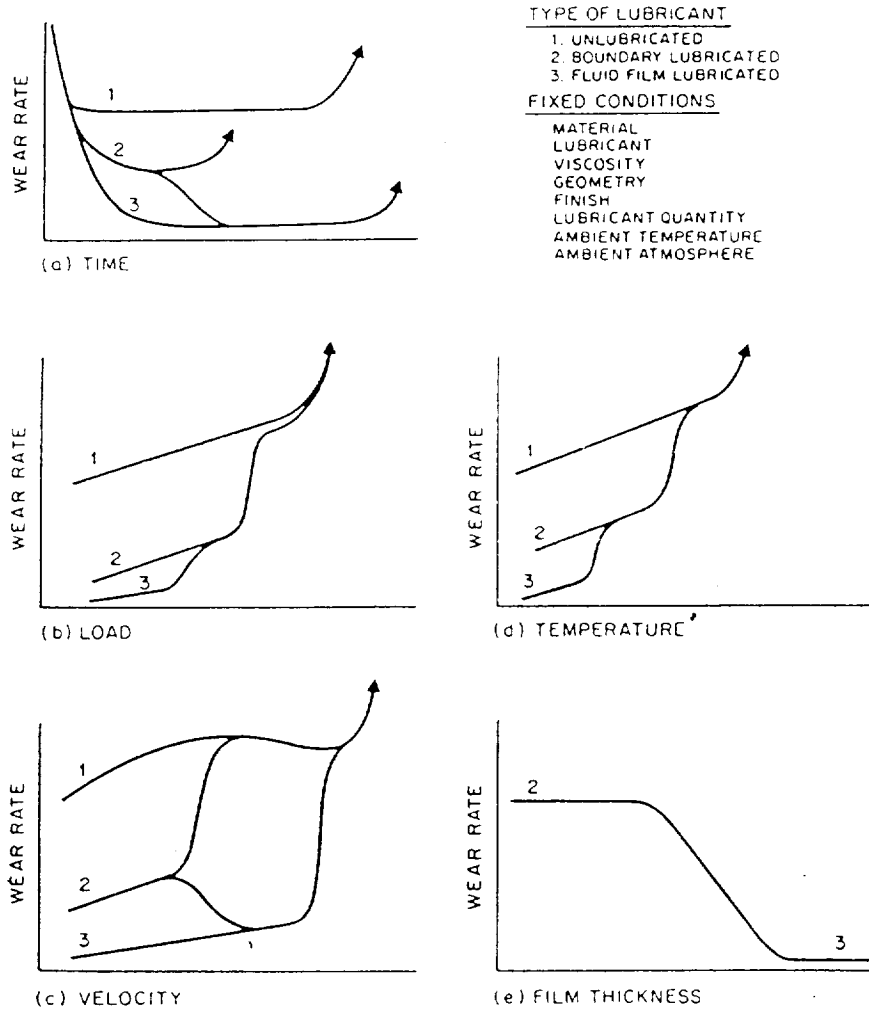


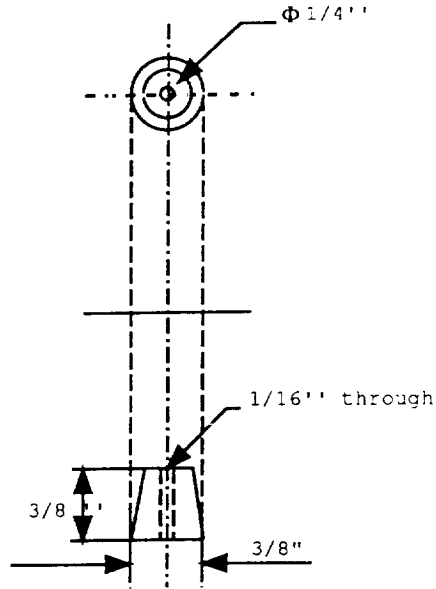
Fig. 12 Effect of Operational Variables on Wear Rate

APPENDIX A

PRELIMINARY DRAWINGS

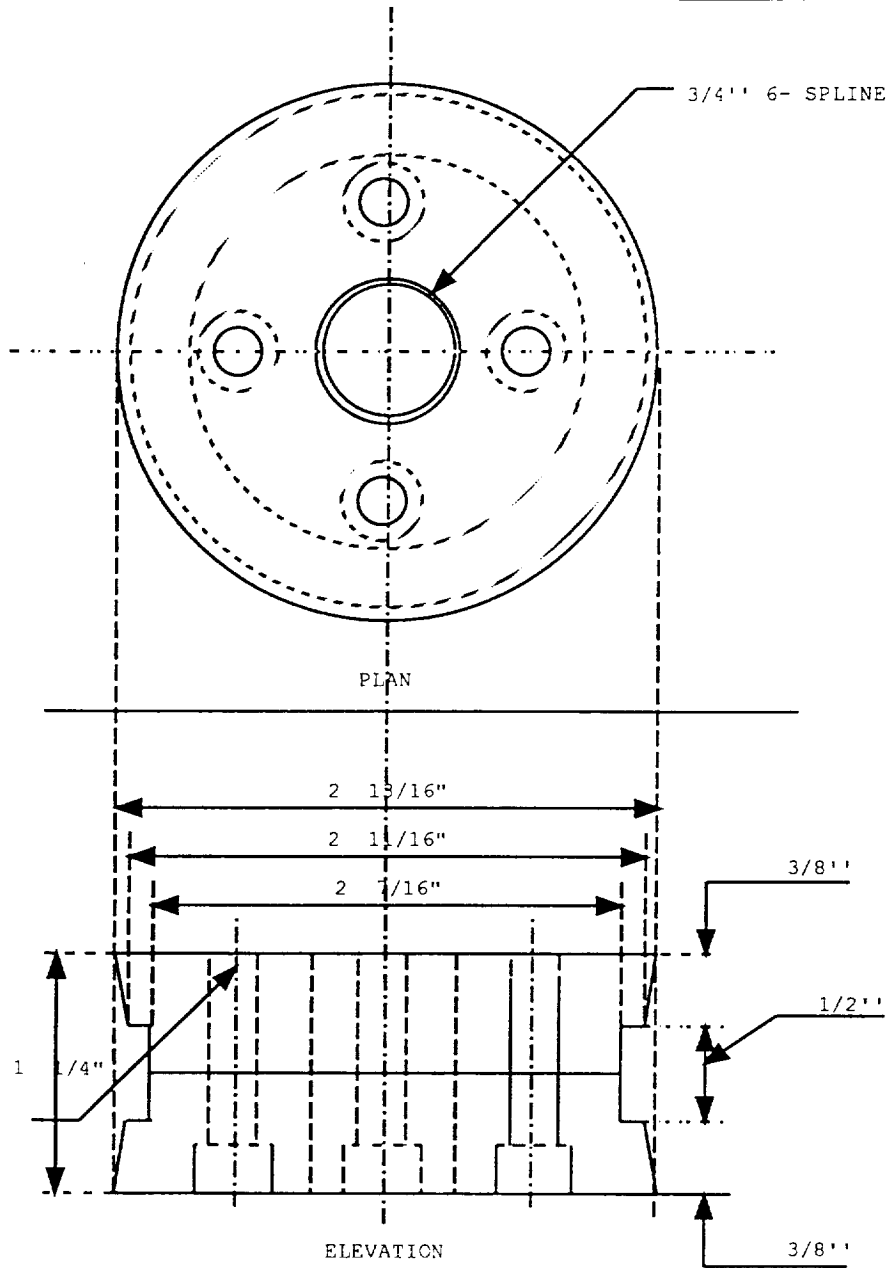
OF

MAGNETOSTRICTIVE DIRECT DRIVE MOTOR



DRIVE ROLLER
 MATERIAL: SAE 52100
 NOS: 32

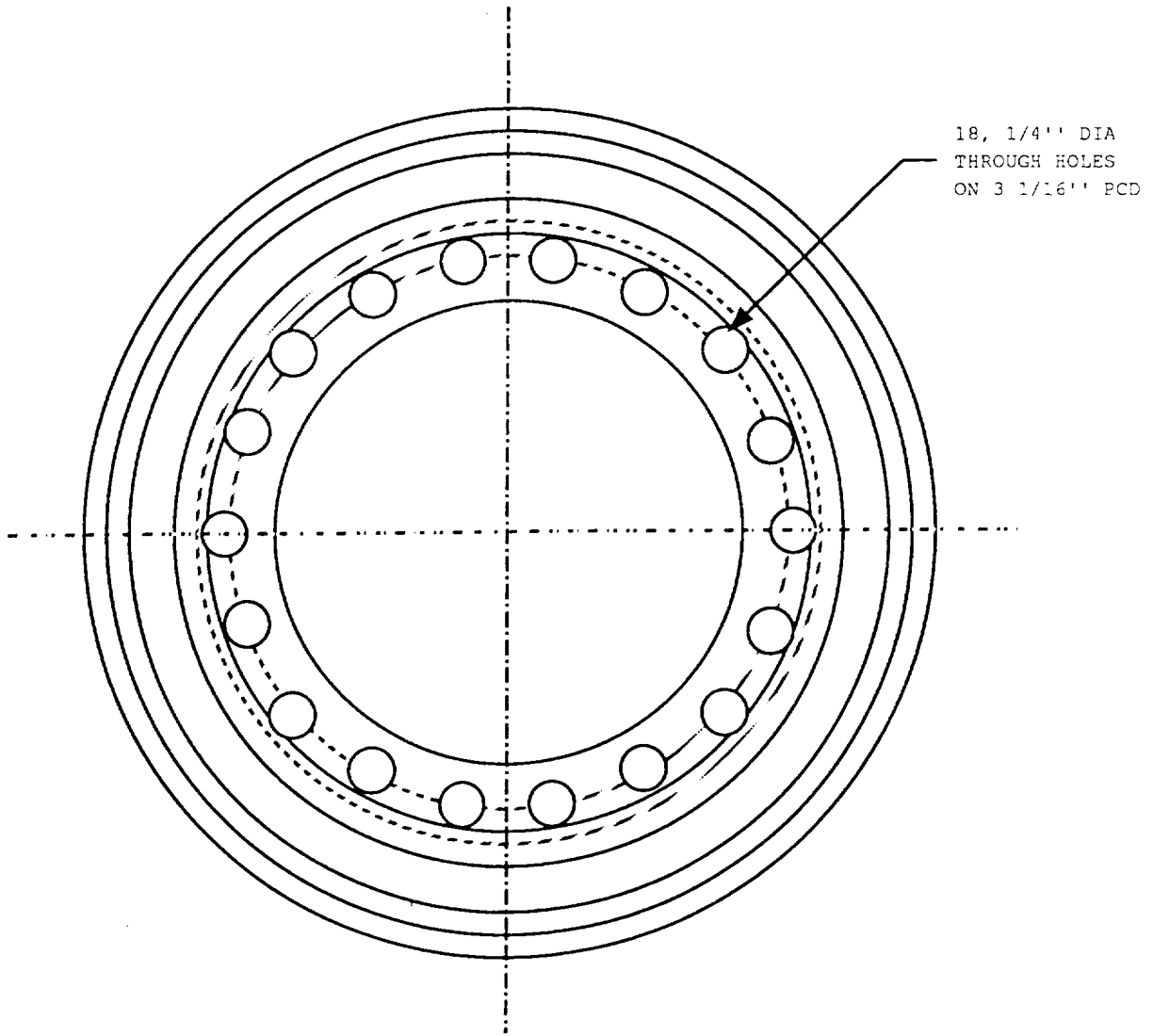
<u>DRIVE ROLLER</u>		SR. NO. 1
DESIGNED BY: JMV	DRAWN BY: DPN	DATE: 8/8/90
SCALE: 1:1		



4 M6*1 SOCKET HEAD
CAP SCREWS

DRIVE SHAFT DRUM
MATERIAL: SAE 52100
NOS: 1

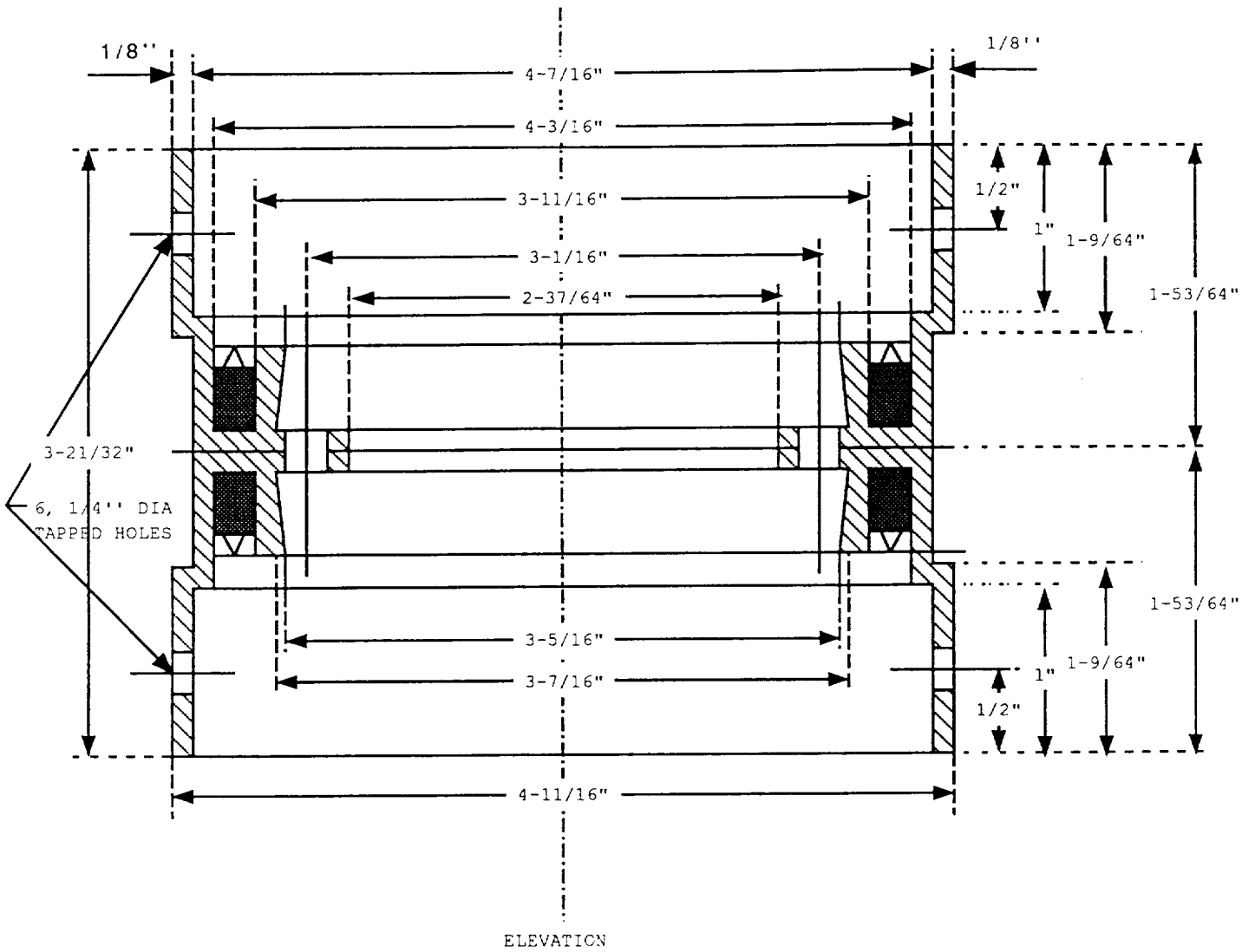
<u>DRIVE SHAFT DRUM</u>		SR. NO. 2
DESIGNED BY: JMV	DRAWN BY: DPN	DATE: 8/8/90
SCALE: 1:1		



PLAN

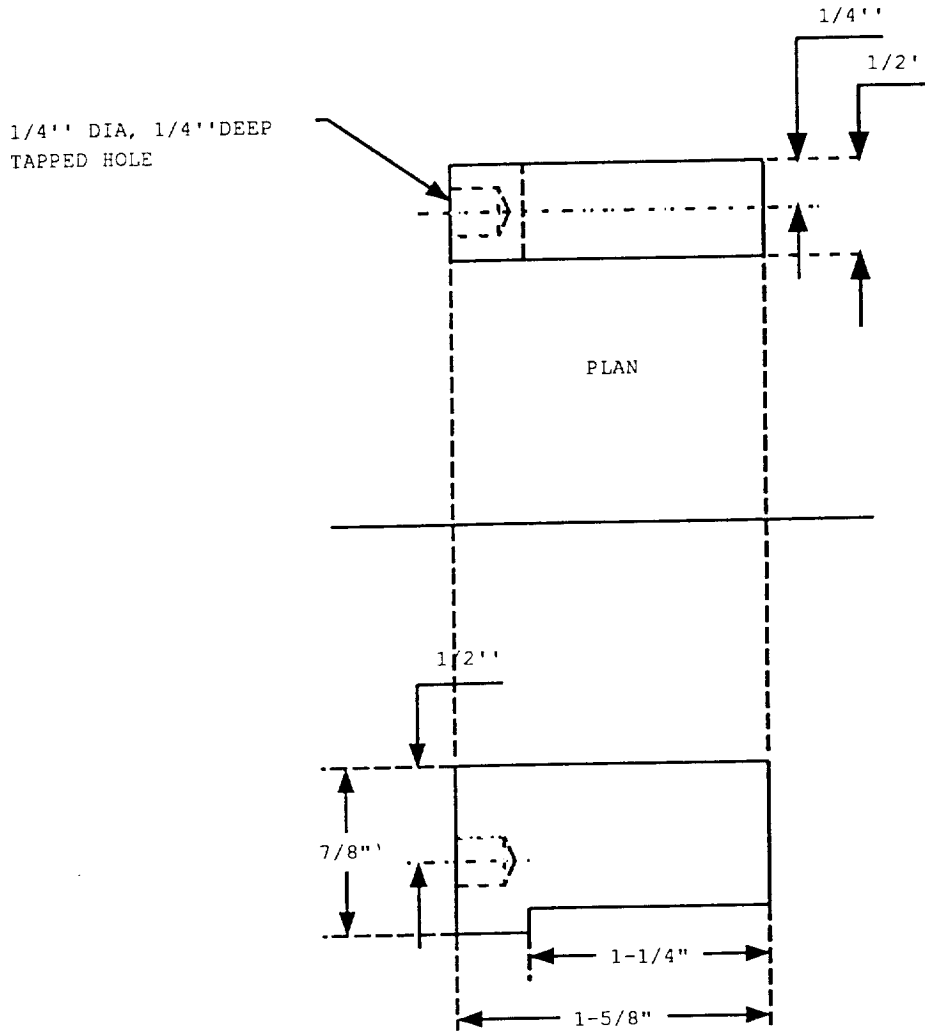
DRIVE DRUM
 MATERIAL: SAE 52100
 NOS: 1

<u>DRIVE DRUM</u>		SR. NO. 3
DESIGNED BY: JMV	DRAWN BY: DPN	DATE: 8/8/90
SCALE: 1:1		

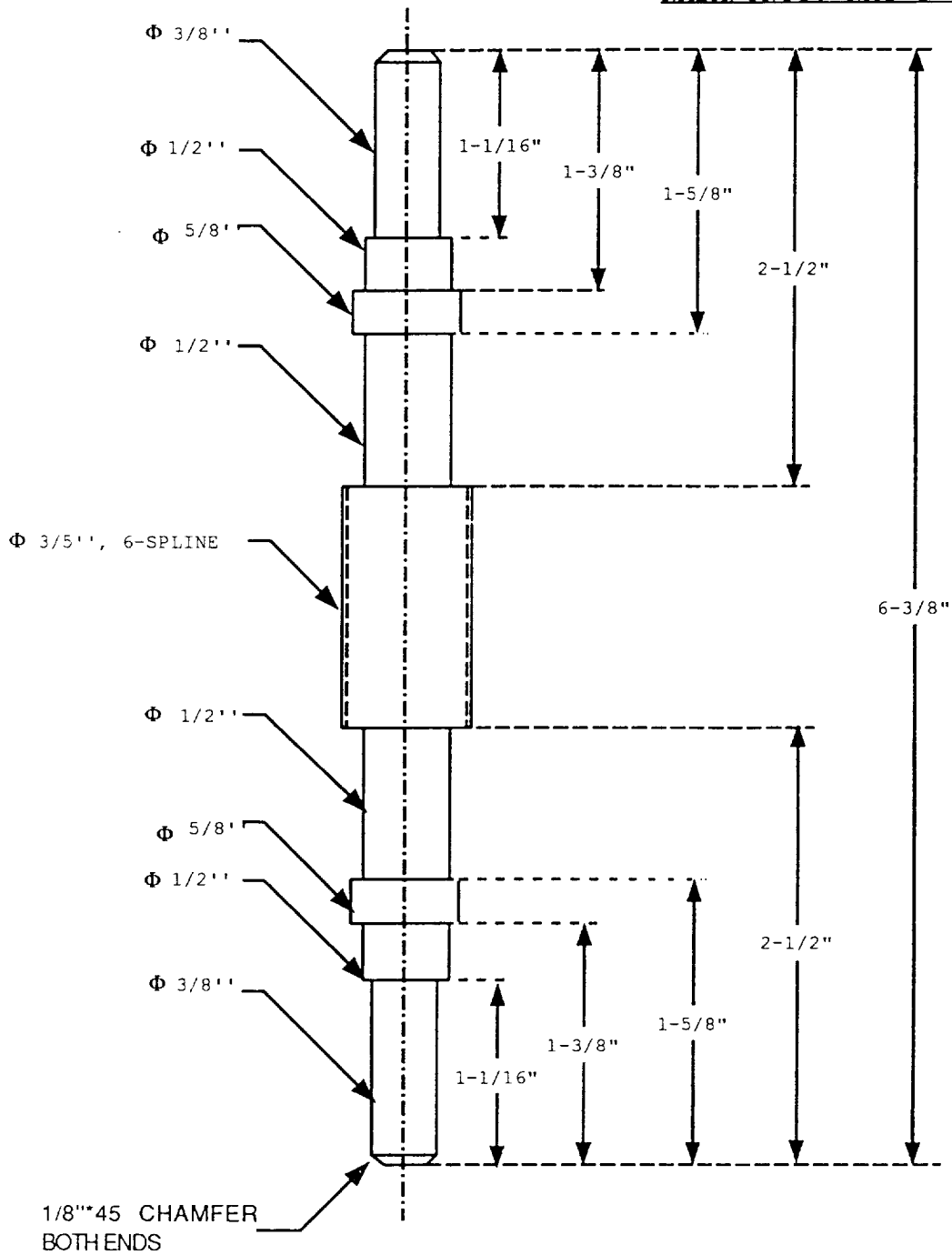


DRIVE DRUM
 MATERIAL: SAE 52100
 NOS: 1

<u>DRIVE DRUM</u>		SR. NO. 3
DESIGNED BY: JMV	DRAWN BY: DPN	DATE: 8/8/90
SCALE: 1:1		

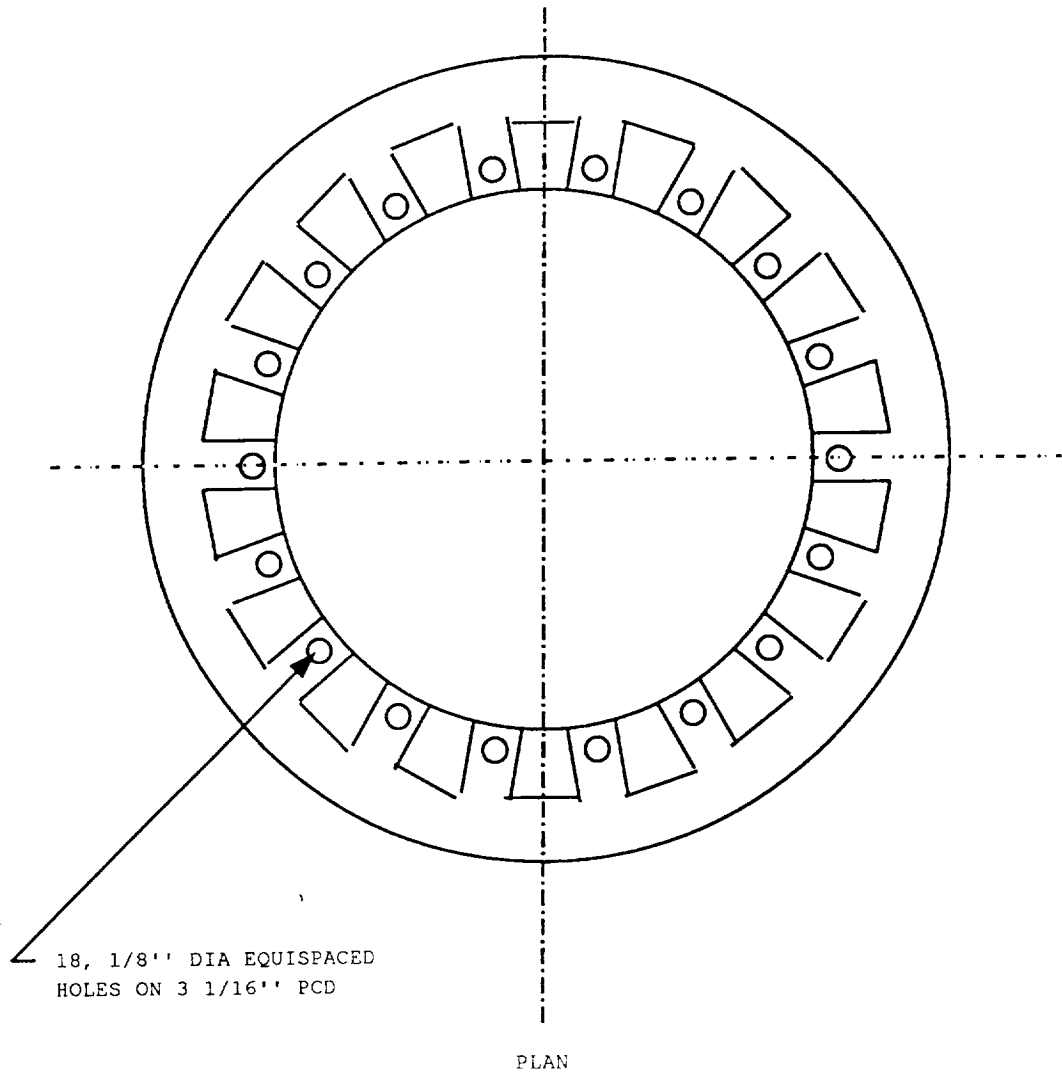


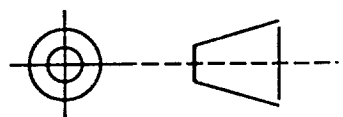
<u>TORQUE ARM PLATE</u>		SR. NO. 4
DESIGNED BY: JMV	DRAWN BY: DPN	DATE: 8/8/90
SCALE: 1:1		

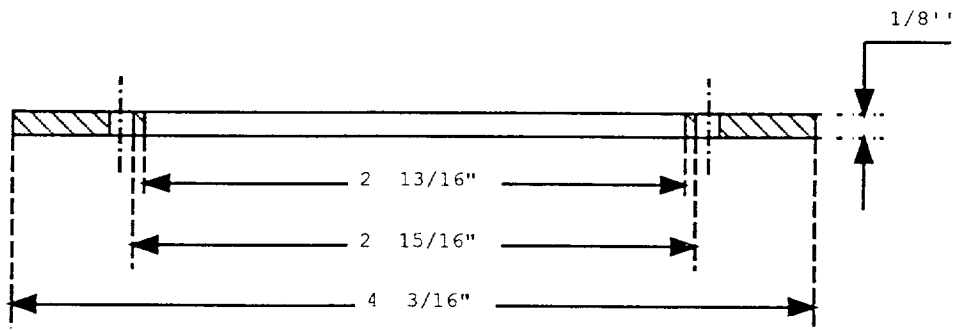


SHAFT
 MATERIAL: SAE 52100
 NOS: 1

<u>DRIVE SHAFT</u>		SR. NO. 5
DESIGNED BY: JMV	DRAWN BY: DPN	DATE: 8/8/90
SCALE: 1:1		

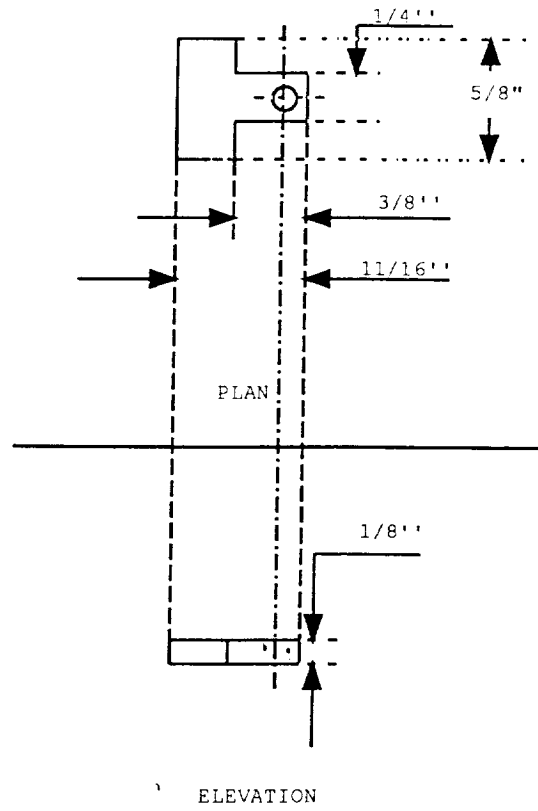


<u>STRIKER PLATE</u>		SR. NO. 6
DESIGNED BY: JMV	DRAWN BY: DPN	DATE: 8/8/90
SCALE: 1:1		



ELEVATION
 STRIKER PLATE
 MATERIAL: SS 316
 NOS: 2

<u>STRIKER PLATE</u>		SR. NO. 6
DESIGNED BY: JMV	DRAWN BY: DPN	DATE: 8/8/90
SCALE: 1:1		

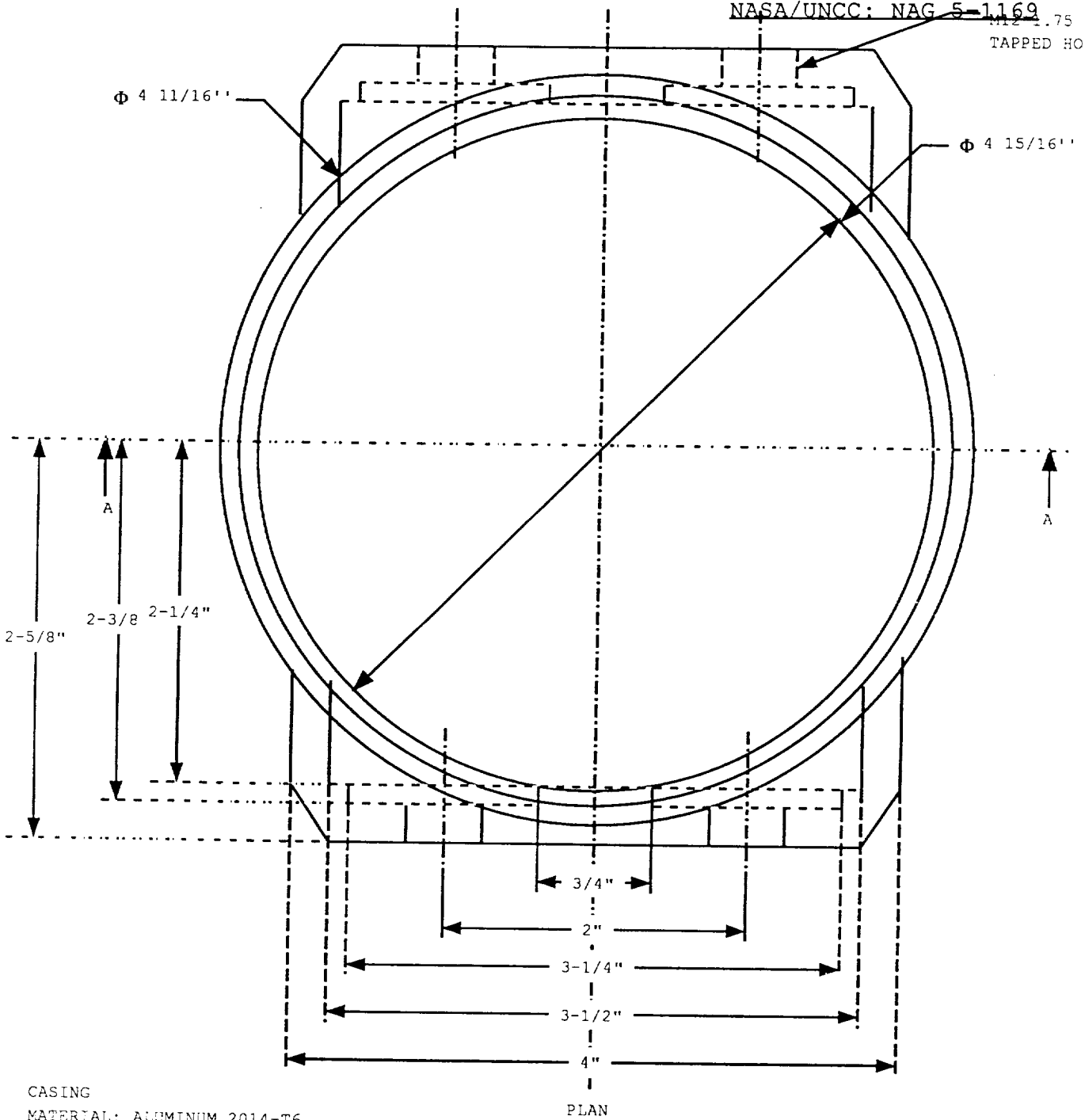


STRIKER DETAILS
MATERIAL: SS 316

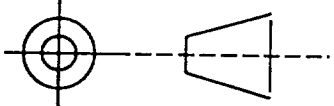
<u>STRIKER DETAILS</u>		SR. NO. 6
DESIGNED BY: JMV	DRAWN BY: DPN	DATE: 8/8/90
SCALE: 1:1		

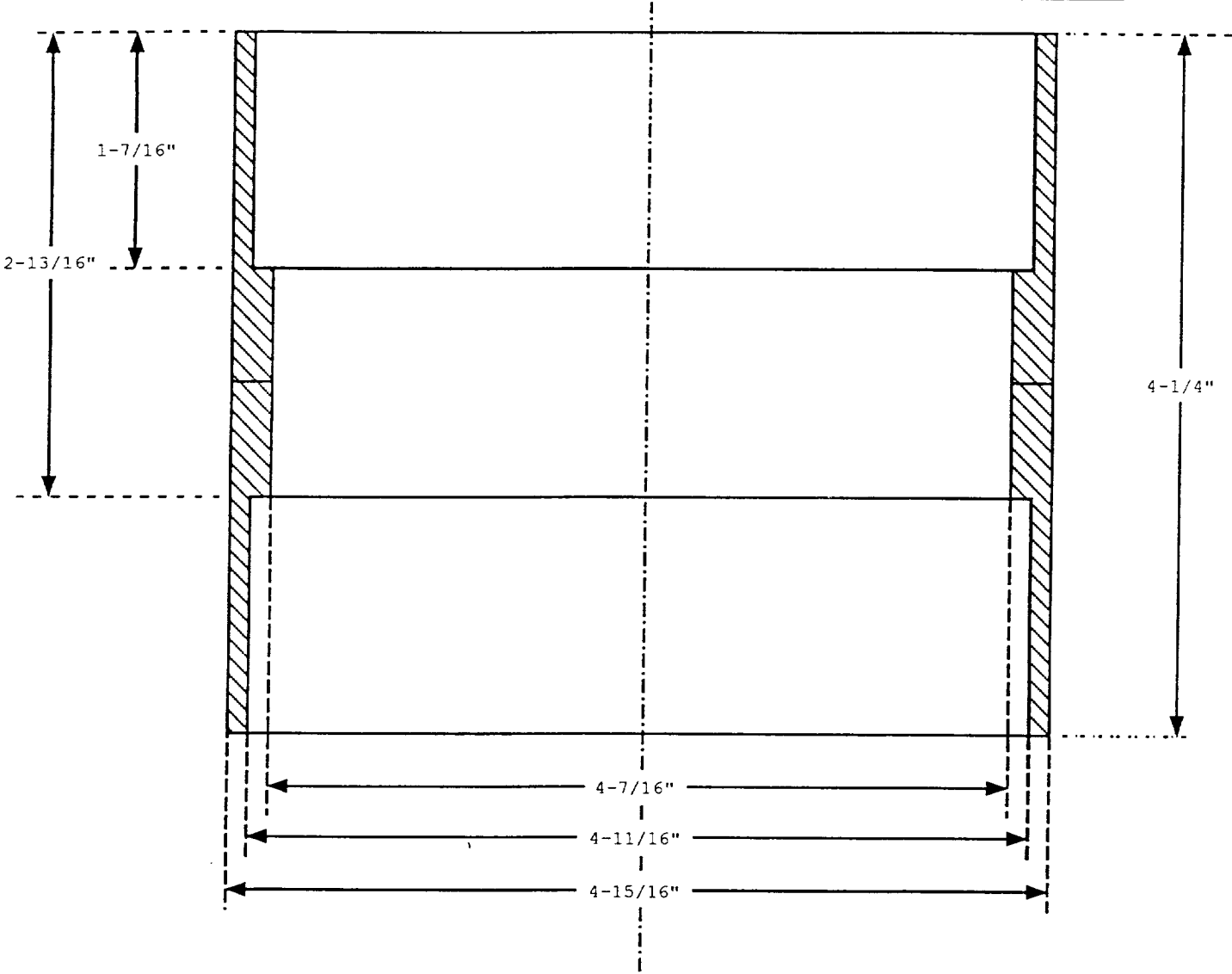
NASA/UNCC: NAG 5-1169

M12 x 1.75
TAPPED HOLE



CASING
MATERIAL: ALUMINUM 2014-T6
NCS: 1

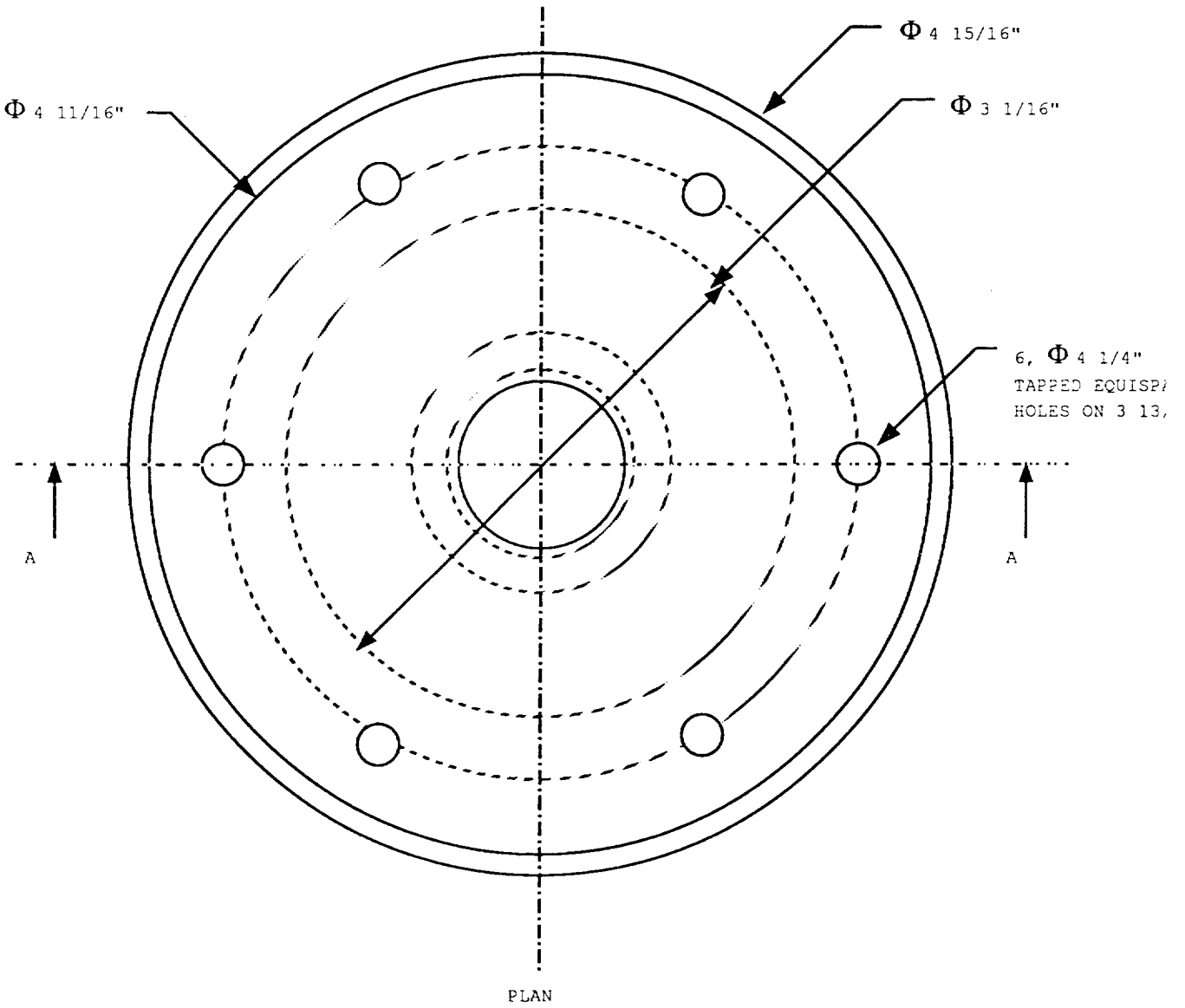
<u>CASING</u>		SR. NO. 7
DESIGNED BY: JMV	DRAWN BY: DPN	DATE: 8/8/90
SCALE: 1:1		



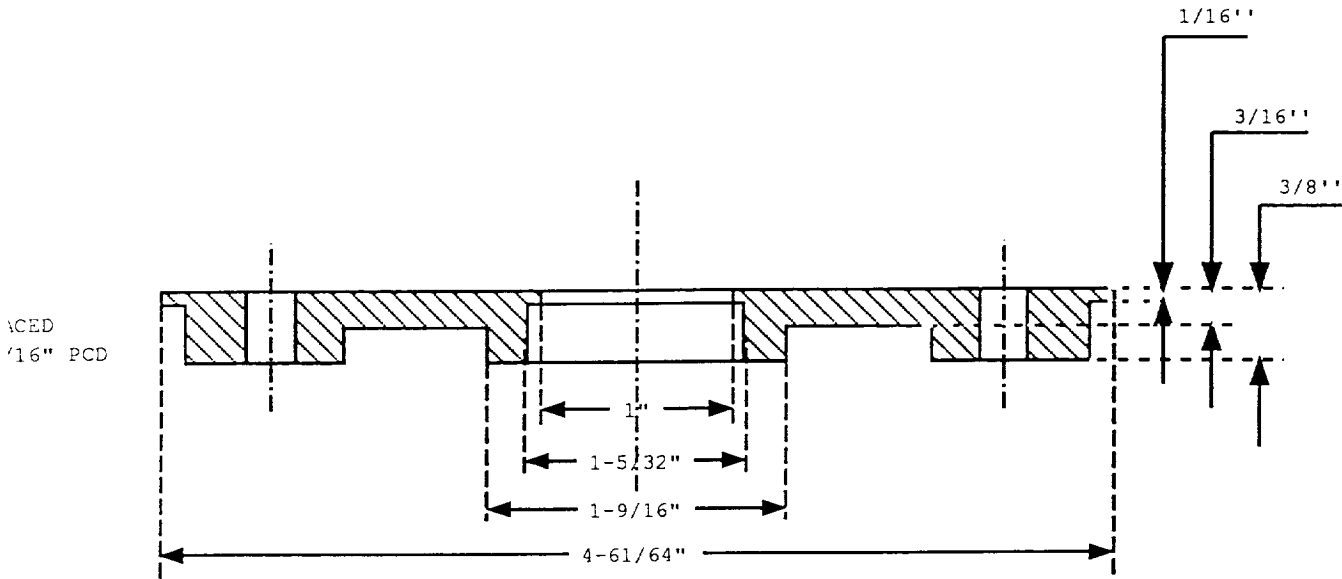
ELEVATION

CASING
 MATERIAL: ALUMINUM 2014-T6
 NOS: 1

<u>CASING</u>		SR. NO. 7
DESIGNED BY: JMV	DRAWNED BY: DPN	DATE: 8/8/90
SCALE: 1:1		



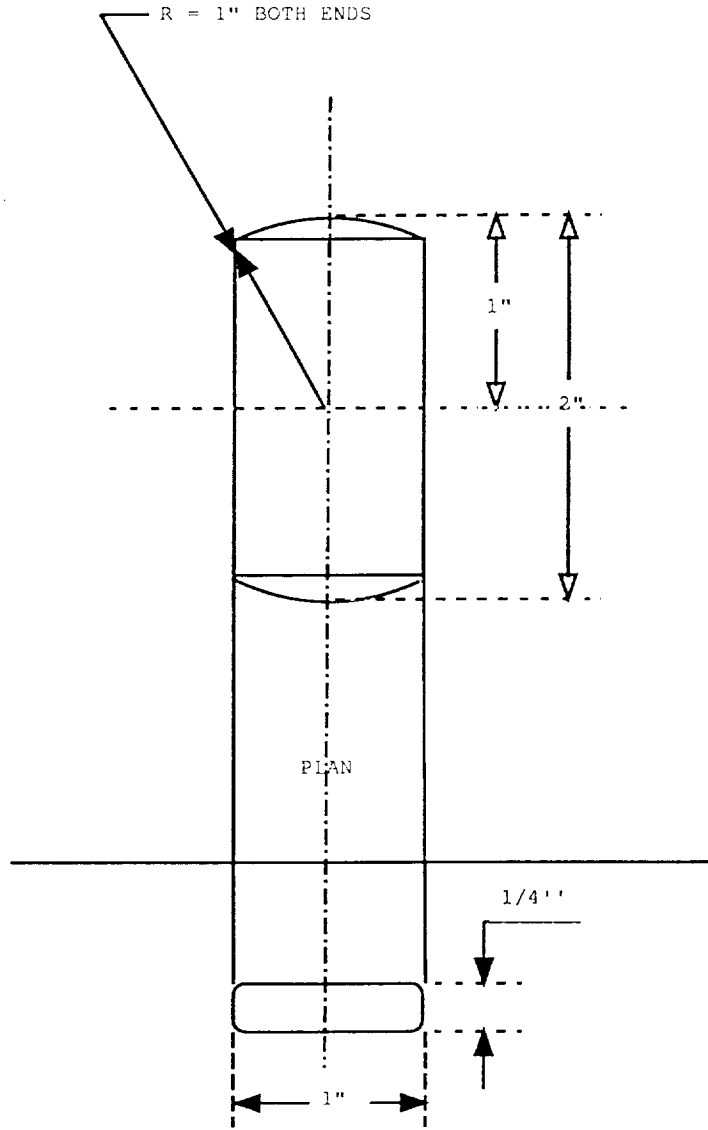
<u>END COVERS</u>		SR. NO. 8
DESIGNED BY: JMV	DRAWN BY: DPN	DATE: 8/8/90
SCALE: 1:1		



SECTION A-A

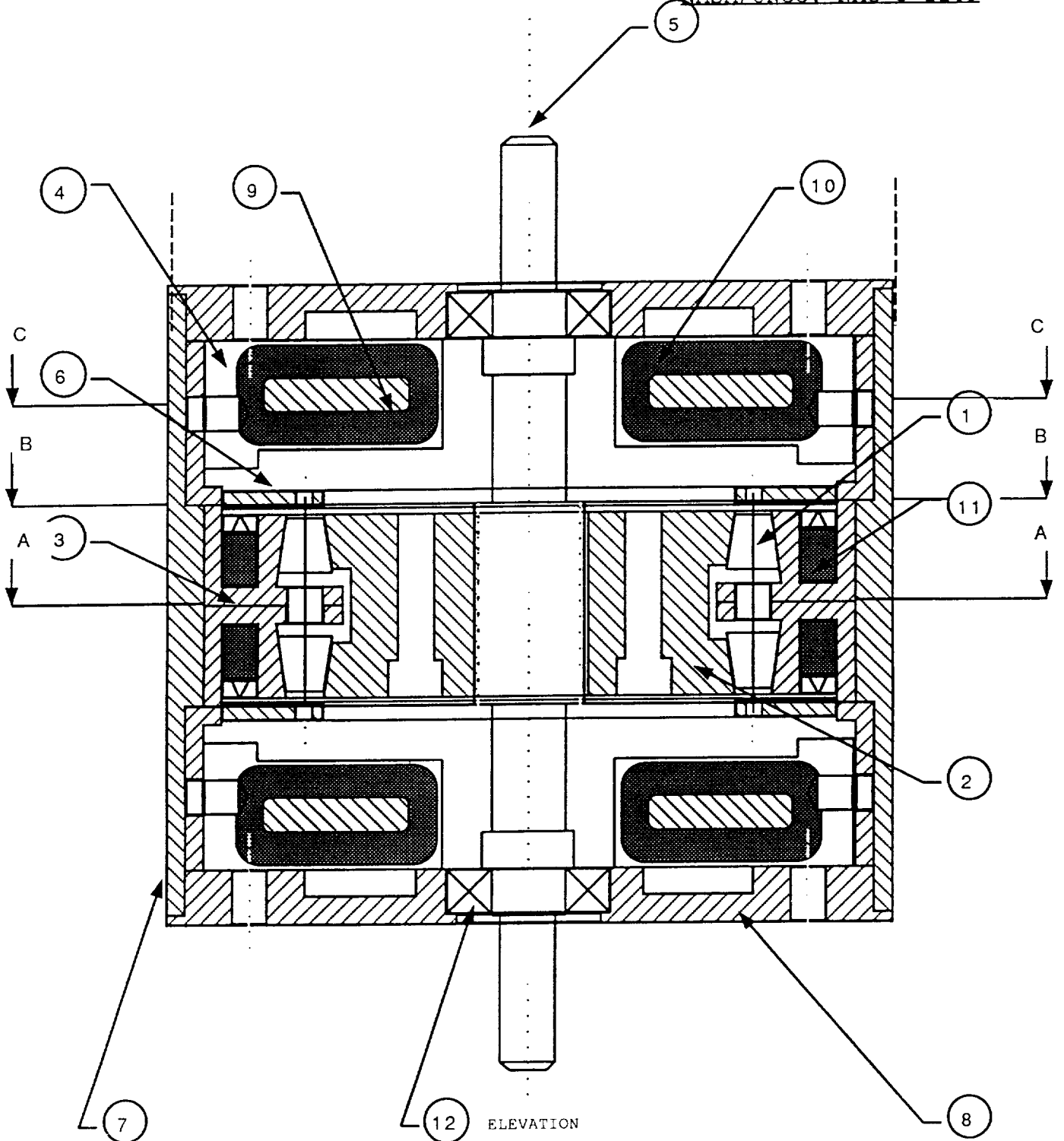
ELEVATION
 END COVER
 MATERIAL: ALUMINIUM
 2014-T6
 NOS: 2

<u>END COVERS</u>		SR. NO. 8
DESIGNED BY: JMV	DRAWNED BY: DPN	DATE: 8/8/90
SCALE: 1:1		

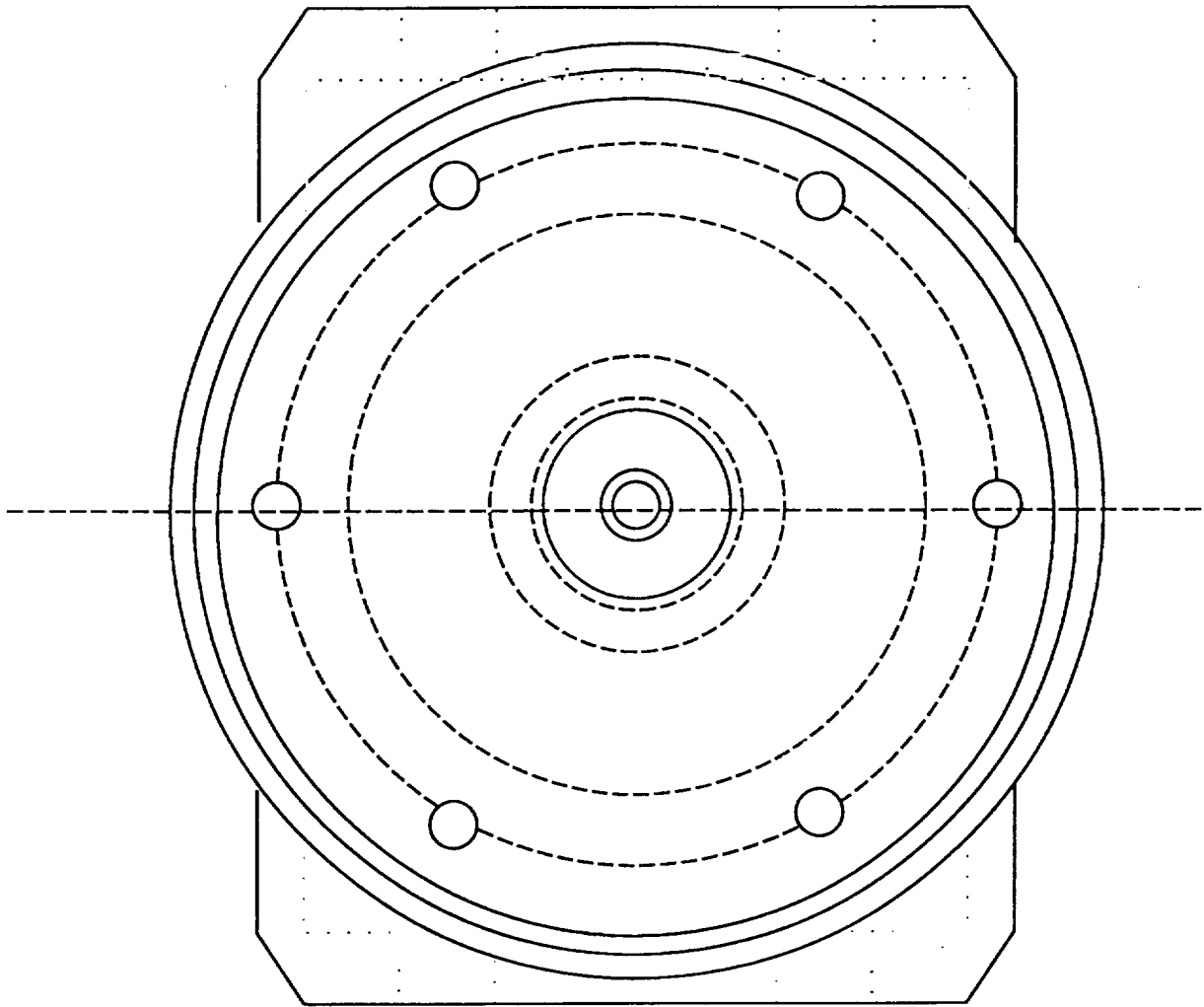


TERFENOL D

<u>TERFENOL RODS</u>		SR. NO. 9
DESIGNED BY: JMV	DRAWN BY: DPN	DATE: 8/8/90
SCALE: 1:1		

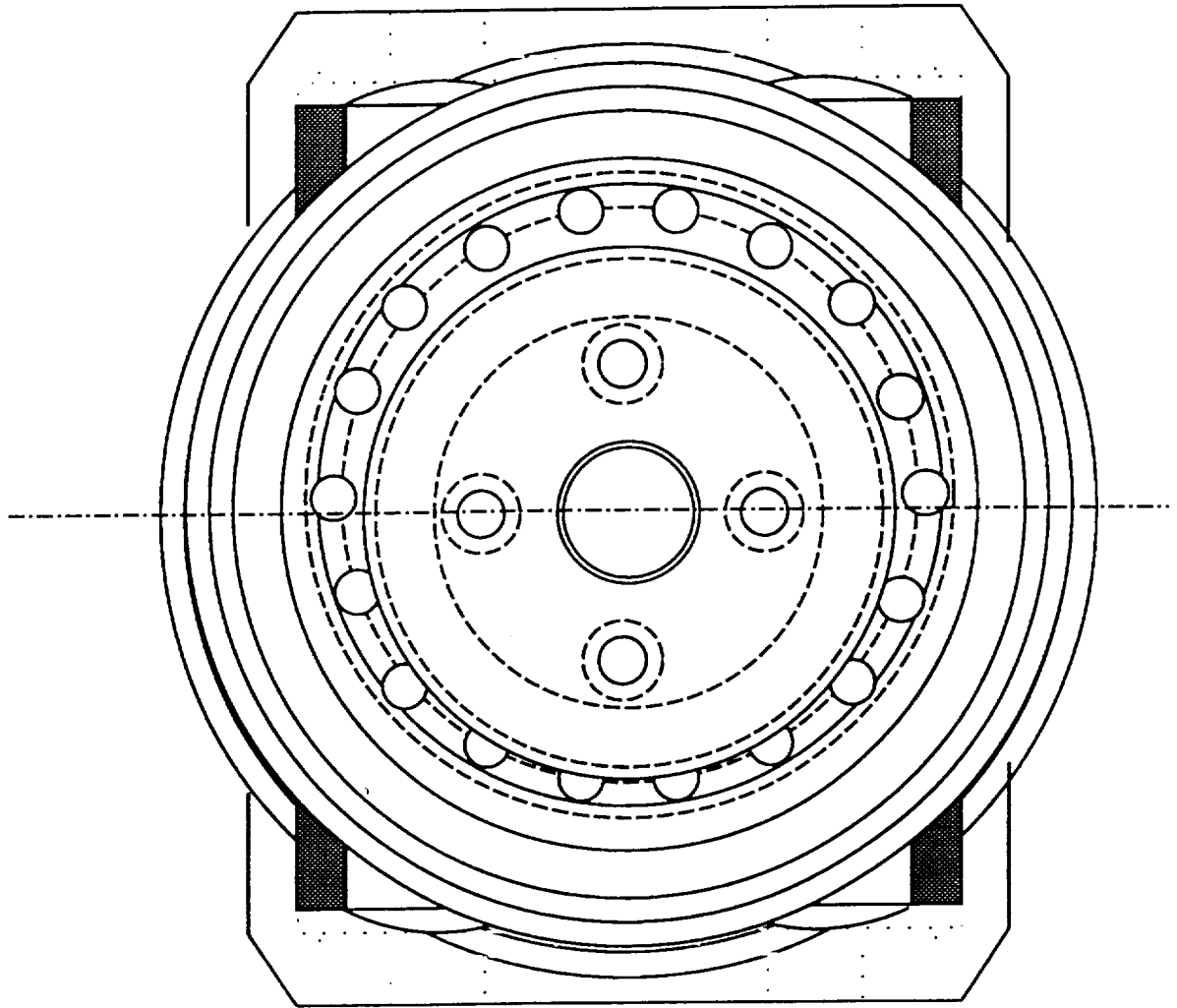


<u>MAGNETOSTRICTIVE DIRECT DRIVE MOTOR (1)</u>		
DESIGNED BY: JMV	DRAWN BY: DPN	DATE: 8/8/90
SCALE: 1:1		



PLAN

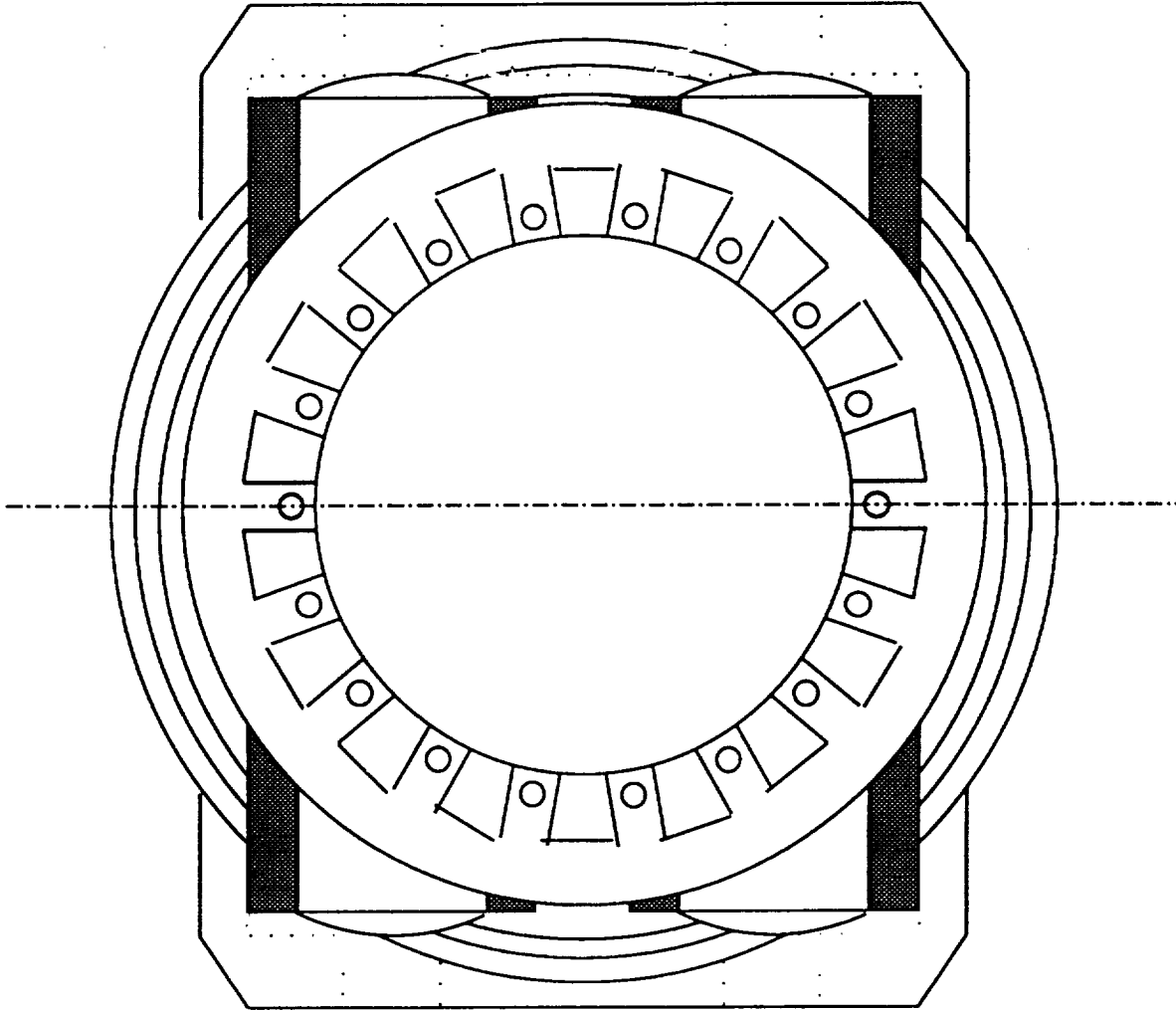
<u>MAGNETOSTRICTIVE DIRECT DRIVE MOTOR (2)</u>		
DESIGNED BY: JMV	DRAWN BY: DPN	DATE: 8/8/90
SCALE: 1:1		



PLAN

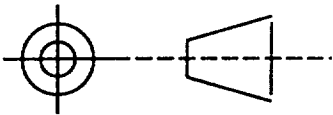
SECTION A-A

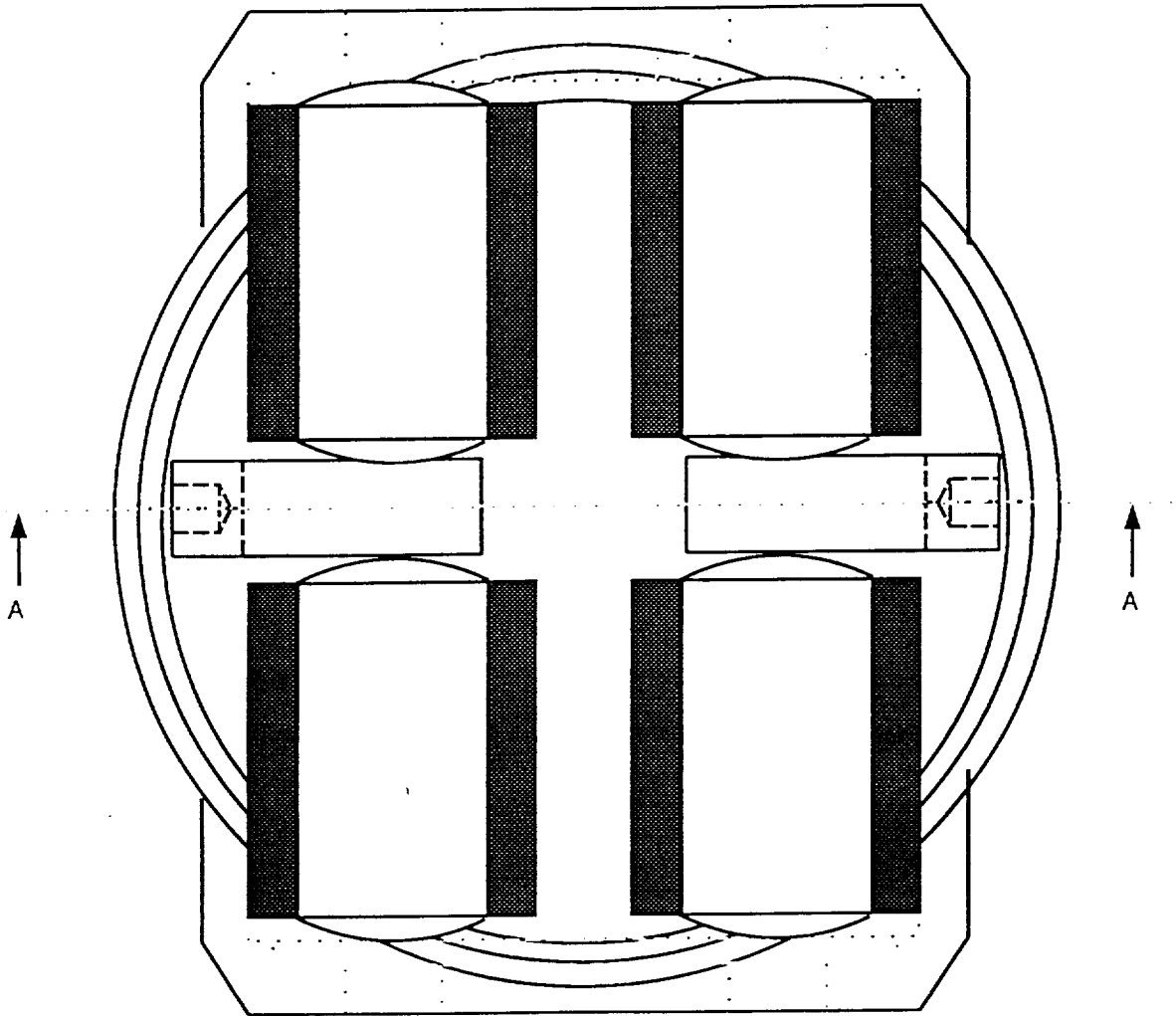
MAGNETOSTRICTIVE DIRECT DRIVE MOTOR (3)		
DESIGNED BY: JMV	DRAWN BY: DPN	DATE: 8/8/90
SCALE: 1:1		



PLAN

SECTION B-B

<u>MAGNETOSTRICTIVE DIRECT DRIVE MOTOR (4)</u>		
DESIGNED BY: JMV	DRAWN BY: DPN	DATE: 8/8/90
SCALE: 1:1		

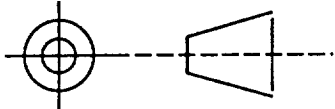


PLAN

SECTION C-C

<u>MAGNETOSTRICTIVE DIRECT DRIVE MOTOR (5)</u>		
DESIGNED BY: JMV	DRAWN BY: DPN	DATE: 8/8/90
SCALE: 1:1		

12	BEARINGS	FAG 6001 2RSR	2
11	ELECTROMAGNETIC COIL	COPPER AWG 23	8
10	DRIVE COILS	COPPER AWG 23	8
9	TERFENOL RODS	TERFENOL D	8
8	END COVERS	ALUMINUM 2014-T6	2
7	CASING	ALUMINUM 2014-T6	1
6	STRIKER PLATE	SS 316	2
5	SHAFT	SS 316	1
4	TORQUE ARM PLATE	SS 316	8
3	DRIVE DRUM	SAE 52100	1
2	DRIVE SHAFT DRUM	SAE 52100	1
1	DRIVE CONE	SAE 52100	36
<u>SR. NO.</u>	<u>DESCRIPTION</u>	<u>MATERIAL</u>	<u>NOS</u>

<u>MAGNETOSTRICTIVE DIRECT DRIVE MOTOR (6)</u>		
DESIGNED BY: JMV	DRAWN BY: DPN	DATE: 8/8/90
SCALE: 1:1		

References

1. Engineering Electromagnetics by William H. Hyat, McGraw-Hill Book Company, Fifth Edition, pp. 298, (1989).
2. Application Manual For The Design of Terfenol-D Magnetostrictive Transducers, Prepared for Edge Technologies, Inc., by Dr. John L. Butler
3. Fein, R.S. : "Equations For The Calculation of The Antiwear Number," Contribution to the Wear Control Handbook by Texaco Inc.